Article

Species-Selective Pyrimidineamine Inhibitors of Trypanosoma brucei S-Adenosylmethionine Decarboxylase

Oleg A. Volkov, Anthony J. Brockway, Stephen A Wring, Michael Peel, Zhe Chen, Margaret A. Phillips, and Jef K. De Brabander

Species-Selective Pyrimidineamine Inhibitors of *Trypanosoma brucei S-Adenosylmethionine Decarboxylase.*

Oleg A. Volkov,[1,&] Anthony J. Brockway,[2,&] Stephen A. Wring,[3] Michael Peel,[3] Zhe Chen,[4] Margaret A. Phillips,[1,2,*] and Jef K. De Brabander[2,*]

Departments of [1]Pharmacology, [2]Biochemistry, and [4]Biophysics, University of Texas Southwestern Medical Center, 5323 Harry Hines Blvd., Dallas, Texas 75390-9038, United States

[3]Scynexis, Inc. (now Avista Pharma Solutions), 3501 Tricenter Boulevard, Suite C, Durham, North Carolina 27713, United States

[&]These authors contributed equally to this work

*Co-corresponding Authors: J.K.D.B. and M.A.P.

Emails: Jef.DeBrabander@UTSouthwestern.edu and Margaret.Phillips@UTSouthwestern.edu

Phones: (214) 648-7808 and (214) 645-6164

1
2
3
4
5
6
7
8
9
10
11
12
13
14
15
16
17
18
19
20
21
22
23
24
25
26
27
28
29
30
31
32
33
34
35
36
37
38
39
40
41
42
43
44
45
46
47
48
49
50
51
52
53
54
55
56
57
58
59
60

Abstract

New therapeutic options are needed for treatment of human African trypanosomiasis (HAT) caused by protozoan parasite *Trypanosoma brucei*. *S*-Adenosylmethionine decarboxylase (AdoMetDC) is an essential enzyme in the polyamine pathway of *T. brucei*. Previous attempts to target this enzyme were thwarted by the lack of brain penetration of the most advanced series. Herein, we describe a *T. brucei* AdoMetDC inhibitor series based on a pyrimidineamine pharmacophore that we identified by target-based high-throughput screening. The pyrimidineamines showed selectivity for *T. brucei* AdoMetDC over the human enzyme, inhibited parasite growth in whole-cell assay, and had good predicted blood–brain barrier penetration. The medicinal chemistry program elucidated structure–activity relationships within the series. Features of the series that were required for binding were revealed by determining the X-ray crystal structure of *Tb*AdoMetDC bound to one analog. The pyrimidineamine series provides a novel starting point for an anti-HAT lead optimization.

Keywords: human African trypanosomiasis, *Trypanosoma brucei*, AdoMetDC, pyrimidineamine, co-crystallization.

Introduction

Human African trypanosomiasis (HAT), also known as sleeping sickness, is caused by the single celled protozoal parasite *Trypanosoma brucei* and is classified by the WHO as a Neglected Tropical Disease (NTD).[1] HAT is transmitted by the tsetse fly to humans and animals where it replicates extracellularly in the blood and lymph causing fever and influenza-like symptoms. Later in infection, the parasite crosses the blood–brain barrier (BBB) and invades the central nervous system (CNS) leading to a variety of neurological symptoms, including disruption of the sleep–wake cycle, coma, and eventual death in most patients.[2] The number of reported cases has declined steadily since peaking in 1998 at nearly 40,000 cases a year.[3, 4] Control and surveillance programs, which include both vector control and identification and treatment of infected individuals, have been credited with this decline.[3] The WHO has targeted HAT for sustainable elimination by 2030;[5] however, the recent discovery that some infected individuals are asymptomatic carriers threatens the elimination program.[6] Additionally, it is now recognized that skin and fat serves as a significant reservoir for the parasites and thus screening of blood underestimates the magnitude of the parasite burden in the endemic communities.[7-9]

Currently approved HAT treatments have significant liabilities hindering efforts to control the disease.[3] Particularly problematic are treatments for the CNS stage of the disease. Nifurtimox–eflornithine combination therapy (NECT) has replaced the poorly tolerated melarsoprol as a front-line therapy against Gambian form of the infection.[10] However, both the high cost of this therapy [10] and its limited efficacy against Rhodesian form of HAT has led to continued use of melarsoprol.[11] Thus, it is recognized that a safer and less expensive therapy is needed that would cure both early- and CNS-stage infections caused by either *T. brucei* subspecies, eliminating the need to stage the disease. There are currently only two drug

candidates in clinical development: oxaborole SCYX-7158[12] and nitroheterocyclic

fexinidazole.[13] Both have the potential to meet the outlined treatment goals but it is too early to

know if either will make it to registration.

Of the approved drugs only eflornithine has a well understood mechanism of action. It

targets ornithine decarboxylase, a key enzyme in polyamine biosynthesis, suggesting that other

enzymes in the pathway would also provide potential targets for drug discovery.[14, 15] A second

key enzyme in the pathway, *S*-adenosylmethionine decarboxylase (AdoMetDC), has been shown

to be essential by genetic studies,[16] and small-molecule inhibitors of AdoMetDC have been

reported that show *in vivo* activity against *T. brucei* in mouse models.[14, 17-19] However, *T. brucei*

AdoMetDC inhibitors, such as CGP 40215, mechanism-based MDL 73811, and its derivative

Genz-644131 (**1**), were deemed unsuitable for anti-HAT development as their physicochemical

properties were not consistent with good blood–brain barrier (BBB) penetration and thus they

were not effective for CNS stage of the disease.[14, 17, 18] AdoMetDCs from trypanosomatids have a

novel subunit configuration that differentiates them from the human enzyme: they are

allosterically activated by heterodimerization with an inactive paralogous pseudoenzyme, we

termed prozyme.[20] Structural analysis by X-ray crystallography demonstrated that

heterodimerization leads to displacement of an autoinhibitory sequence and to a coupled

structural reorganization that stabilizes the active conformation through insertion of the N-

terminus into the heterodimer interface.[21] These structural differences suggested that selective

inhibition of the parasite enzyme over the host enzyme was plausible.

We recently described mass spectrometry-based high-throughput screening (HTS) campaign

that identified 13 classes of novel small-molecule inhibitors of *T. brucei* AdoMetDC that also

inhibited parasite growth.[22] Several of the identified series demonstrated high propensity to cross

the BBB and were at least partially on-target in the parasite cells.[22] Herein, we characterize a

pyrimidineamine chemotype that was identified as a hit in the HTS. Initially, the hit failed to

demonstrate substantial AdoMetDC inhibition in validation studies and thus was not previously

reported. We later discovered that the potency of the initial hit compound was pH-dependent,

triggering re-prioritization of the pyrimidineamines for a medicinal chemistry effort to establish

the structure–activity relationships (SAR) within the series. A number of pyrimidineamine

analogs with low-micromolar activity on both the enzyme and the parasites were identified.

Compounds in the series also showed good selectivity versus the human enzyme and were

predicted to cross the blood–brain barrier. Finally, a crystal structure of *Tb*AdoMetDC bound to

one analog was determined, providing insight into the structural basis for the pH dependence of

inhibitor binding to *T. brucei* AdoMetDC, and paving the way for future lead development. This

work has led to the validation of the pyrimidineamines as a hit series that could be taken forward

into a hit-to-lead optimization program for the treatment of HAT.

Results

Synthesis. Compound **7** was purchased from Maybridge (part of Thermo Fisher Scientific),

and compounds **56-59**, **74-88**, and **90** were purchased from ChemBridge (San Diego, CA, USA).

The synthesis of all other analogs is shown in Scheme 1.

Results

Synthesis. Compound **7** was purchased from Maybridge (part of Thermo Fisher Scientific),

and compounds **56-59**, **74-88**, and **90** were purchased from ChemBridge (San Diego, CA, USA).

The synthesis of all other analogs is shown in Scheme 1.

Scheme 1. Synthesis of pyrimidineamines[a]
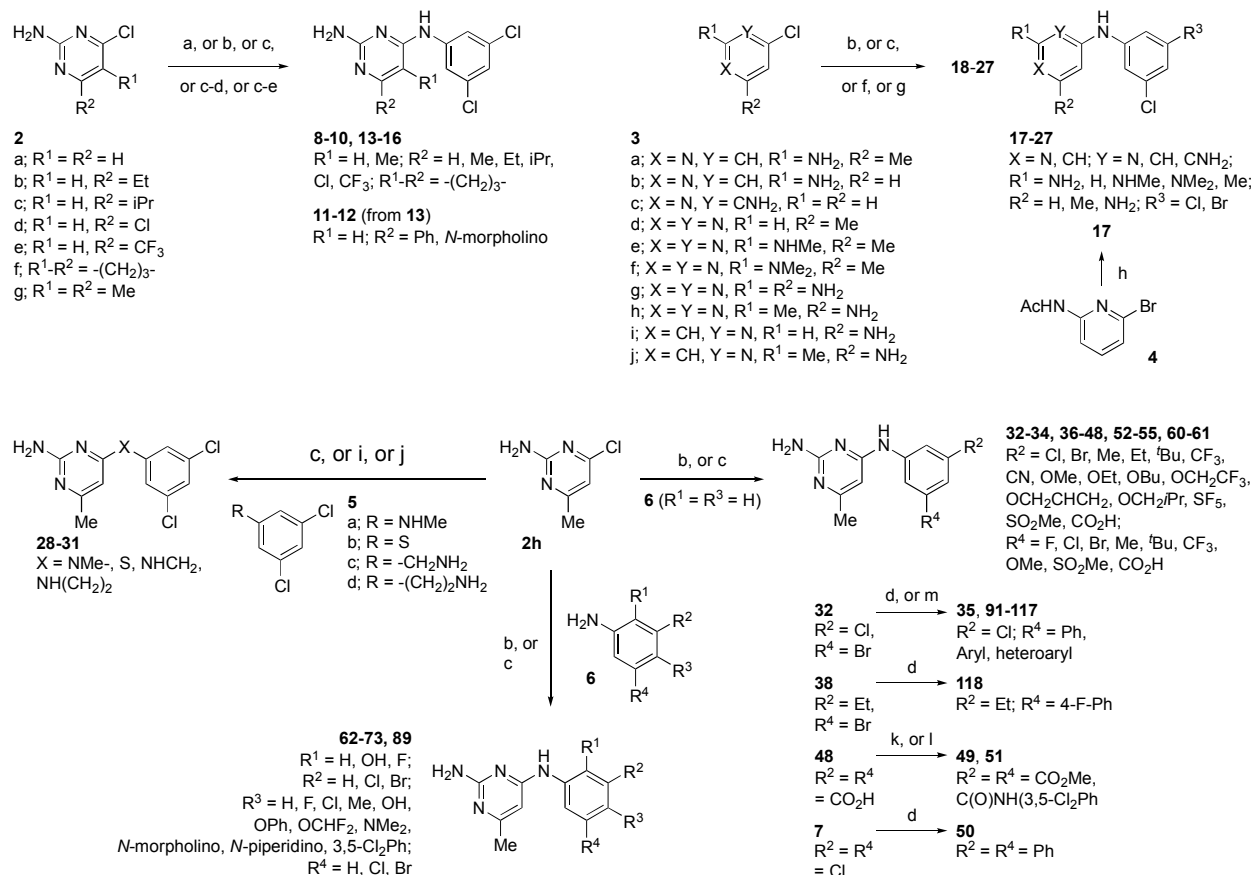
[a] Reagents and conditions: (a) **2a**, 3,5-Cl$_2$PhNH$_2$, DMSO, 100 °C, 18 h (**8**); (b) **2a-c,f-h** or

3g, aniline (3,5-Cl$_2$PhNH$_2$ or 3-Br-5-ClPhNH$_2$ or **6**), conc. HCl, EtOH, microwave (140 °C), 1.5

h (**9**, **10**, **15**, **16**, **26**, **32-34**, **36**, **37**, **44**, **45**, **53**, **54**, **61-68**, **72**, **73**, **89**); (c) **2a,d,e,h** or **3d-f,h**,

aniline (3,5-Cl$_2$PhNH$_2$ or 3-Br-5-ClPhNH$_2$ or **5a** or **6**) conc. HCl, EtOH, reflux, 18 h (**13**, **14**,

23-25, **27**, **28**, **38-43**, **46-48**, **52**, **55**, **60**, **69-71**); (d) **7** or **13** or **32** or **38**, ArylB(OH)$_2$, Pd(OAc)$_2$,

PPh$_3$, Na$_2$CO$_3$, H$_2$O/DME, 90 °C, 18 h (**11**, **35**, **50**, **91-109**, **116-118**); (e) **13,** DIPEA,

morpholine, CH_3CN, microwave (140 °C), 2 h (12); (f) 3,5-Cl_2PhNH_2, **3a,c,i,j,** conc. HCl,

BuOH, microwave (185 °C), 4 h (**18-20**, **22**); (g) 3,5-Cl_2PhNH_2, **3b**, conc. HCl, MeOH/H_2O

(1/1), sealed tube, 100 °C, 18 h (**21**); (h) **4**, 3,5-Cl_2PhNH_2, cat. $Pd_2(dba)_3$, BINAP, NaO^{t}Bu,

toluene, 70 °C, 18 h; then 3N aq. NaOH, EtOH, reflux, 18 h (**17**); (i) **2h**, **5b**, Et_3N, DMF, rt, 24 h

(**29**); (j) **2a**, **5c,d**, DIPEA, CH_3CN, microwave (140 °C), 2 h (**30**, **31**); (k) **48**, conc. H_2SO_4,

MeOH, 4Å mol. sieves, reflux, 18 h (**49**); (l) **48**, 3,5-Cl_2PhNH_2, EDI, py/DCM/DMF (0.4/1/1), rt,

18 h (**51**); (m) **32**, heteroaryl boronic acid MIDA-ester, cat. $Pd(OAc)_2$, PPh_3, sodium

triphosphate, dioxane/H_2O) (4/1), 90 °C, 18 h (**110-115**).

Compounds **9-10**, **13-16**, **18-28**, **32-34**, **36-48**, **52-55**, **60-73**, and **89** were readily available

via reaction of the appropriate chloropyrimidine (**2a-h**, **3d-h**) or chloropyridine (**3a-c**, **3i-j**) with

a variety of substituted anilines in the presence of acidic ethanol or butanol under conventional[23]

or microwave heating.[24] Compound **8** was obtained similarly but under neutral conditions via

heating of chloropyrimidine **2a** with 3,5-Cl_2PhNH_2 in DMSO at 100 °C, whereas amine-linker

analogs **30-31** resulted from microwave heating of chloropyrimidine **2h** with amines **5c-d** in

acetonitrile in the presence of ^{i}Pr$_2$NEt.[25] Stirring thiol **5b** with chloropyrimidine **2h** and

triethylamine in DMF at room temperature yielded thioether-linked analog **29**.[26] Analog **12** was

obtained from chloride-displacement in **13** with morpholine in the presence of ^{i}Pr$_2$NEt under

microwave heating in acetonitrile.[27] The bis-ester and amide analogs **49** and **50** resulted from

Fisher esterification and EDI-mediated amide coupling of **48**, respectively. Pyridine analog **17**

was obtained via palladium-catalyzed amination of pyridinylbromide **4** with 3,5-Cl_2PhNH_2

followed by base-mediated hydrolysis of the acetamide.[28] Finally, all biaryl-containing

compounds (**11**, **35**, **50**, **91-118**) were prepared via Suzuki cross-coupling of the corresponding

arylchloride (**7**, **13**) or arylbromide (**32**, **38**) analogs with arylboronic acids[29] or the corresponding MIDA boronates.[30]

Discovery of pyrimidineamines as *T. brucei* AdoMetDC inhibitors. The pyrimidineamine **7** was identified as a singleton in our previously reported HTS campaign to identify inhibitors of *Tb*AdoMetDC (Figure 1A).[22] Compound **7** did not comprise substructural motifs characteristic of pan-assay interference compounds (PAINS),[31] according to our analysis performed as described in ref 22. The compound was repurchased and tested for inhibition of *T. brucei* cell growth in vitro demonstrating a half-maximal effective growth-inhibitory concentration (EC$_{50}$) of 5.6 μM after 48 h treatment. However, retesting of the *Tb*AdoMetDC enzyme activity yielded a half-maximal inhibitory concentration (IC$_{50}$) of 30 μM (assay pH 7.7). Thus, the compound was not presented in the original HTS publication, where the IC$_{50}$ threshold for an active hit was set at 25 μM.

Later, characterization of the pH dependence of the *Tb*AdoMetDC inhibition profile showed that there was a 60-fold increase in inhibitory activity of **7** at pH 6.8 compared with pH 7.7 (Figure 1B; IC$_{50}$ = 30, 3.7, and 0.50 μM at pH 7.7, 7.2, and 6.8, respectively). The pK_a value of the conjugated acid of the aromatic nitrogen in position 1 (further denoted as pK_a(N1)) was estimated using *MarvinSketch* (version 16.3.28.0, ChemAxon, Budapest, Hungary) to be 7.3 (Figure 1A). Thus, we hypothesized that protonation of N1 in **7** was important for binding to the *T. brucei* AdoMetDC. Pyrimidineamine analogs (described below) with predicted pK_a(N1) of 7.3 had similar slopes of IC$_{50}$–pH dependence, while analogs with pK_a(N1)) > 9 had much shallower slopes reflecting more comparable percentages of protonated species among the three pH points (Figure 2B). IC$_{50}$ values for the structurally unrelated **1** tested as a control were not appreciably

pH-dependent, as only a 2-fold difference was observed between potencies at pH 6.8 and pH 7.7 (Figure 2B).

Encouragingly, compound **7** was predicted to have a high likelihood for the ability to cross the BBB as assessed using an MDCKII-hMDR1 monolayer cell assay in the presence or absence of P-glycoprotein 1 (Pgp) inhibitor *N*-(4-(2-(6,7-dimethoxy-3,4-dihydroisoquinolin-2(1*H*)-yl)ethyl)phenyl)-5-methoxy-9-oxo-9,10-dihydroacridine-4-carboxamide (GF120918). The assay was performed as previously described.[22] The apparent permeability of **7** was 135 nm/s ± inhibitor, suggesting that **7** is not a substrate of Pgp-mediated efflux. This permeability rate is close to an ideal threshold value of 150 nm/s cited as an indicator of a good likelihood that the compound will cross into the CNS.[32]
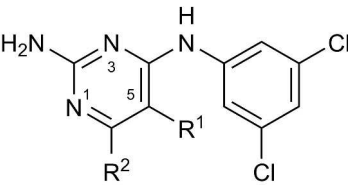
Mechanism of inhibition studies. Reversibility of inhibition by **7** was tested in a rapid dilution assay.[33] *Tb*AdoMetDC was equilibrated with **7** (36 µM ~ IC$_{90}$ at pH 7.2) for 30 min and then diluted 100-fold to a concentration that was no longer inhibitory ($<$IC$_{10}$) into reaction buffer containing ~K$_m$ concertation (50 µM) of substrate, *S*-adenosyl-L-methionine (AdoMet), to initiate the reaction. Aliquots were taken out at 5 min intervals, enzyme was quenched, and produced decarboxylated AdoMet (dcAdoMet) was quantified using RapidFire–mass spectrometry (MS) (Figure 2A). The data were compared with those obtained for the vehicle control. Enzyme activity was fully recovered after diluting out the inhibitor following the 30 min treatment, which is consistent with rapidly reversible inhibition.

To determine the modality of the reversible inhibition, we followed dcAdoMet produced at varied concentrations of AdoMet and **7**. The double-reciprocal Lineweaver–Burk plot of the substrate titrations at four inhibitor concentrations is consistent with the competitive inhibition (K$_i$ = 2.6 (2.2–3.0) µM; 95% confidence interval in parentheses) (Figure 2B).

Hit expansion and development of structure–activity relationships (SAR). On the basis of a tractable chemotype and anticipated BBB permeability, **7** was prioritized for a hit-to-lead expansion. The atomic structure of *Tb*AdoMetDC was not available at the start of this project. Thus, the medicinal chemistry effort to elucidate the SAR relied on iterative structure alterations informed by enzyme and *T. brucei* cell-based assays. AdoMetDC inhibitory activity was determined at three pH values (6.8, 7.2, and 7.7) to assess the importance of N1 protonation for binding; only pH 7.2 data are reported in the main text figures and tables. Data collected at the alternative pH values are provided in Supplemental Information (Table S1). Additionally, the inhibition of *Hs*AdoMetDC at pH 7.2 was measured to assess parasite–host enzyme selectivity.

SAR studies: pyrimidine ring substituents. We began the SAR studies by modifying the pyrimidine ring (Table 1). Replacement of the methyl-substituent at C6 with ethyl (**9**) did not disrupt activity in the enzyme or cell-based assays, while increasing bulk at C6 by addition of isopropyl (**10**) led to a ~3-fold increase in the IC_{50} for AdoMetDC inhibition, as did C5–C6 cyclization (**15**) or removal of the C6-Me (**8**). Introduction of aromatic (**11**), heterocyclic (**12**), or electronegative (**13**, **14**) functionality at C6 caused a sharp reduction in inhibitor potency. It is unclear whether this drop is due to steric hindrance, adverse effect on the N1 protonation at the assay pH, or a combination of both. Notably, there was a lack of a corresponding drop in the cell growth assay, suggesting off-target activity. C5 could be methylated (**16**) without loss of enzyme inhibitory activity.
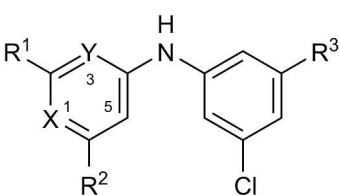
Table 1. SAR of pyrimidine C5 and C6 positions

Compound	R^1	R^2	$pK_a(N1)^a$	Tb IC$_{50}$,^{b} μM	Hs IC$_{50}$,^{c} μM	Tb427 EC$_{50}$,^{d} μM
7	H	Me	7.3	3.7 (3.3–4.1)	27% at 180	5.6 (4.5–7.1)
8	H	H	6.6	13 (11–15)	>180	9.9 (7.7–13)
9	H	Et	7.1	3.0 (2.7–3.3)	36% at 180	4.7 (4.1–5.4)
10	H	^{i}Pr	7.0	12 (10–14)	>180	4.7 (3.9–5.8)
11	H	Ph	6.1	24% at 21	>21	7.2 (6–8.5)
12	H	*N*-morpholino	6.0	>180	>180	13 (10–17)
13	H	Cl	–2.2	>180	>180	8.9 (7.3–11)
14	H	CF$_3$	–3.3	>180	>180	10 (7.5–14)
15		-(CH$_2$)$_3$-	6.8	12 (11–14)	>21	19 (15–24)
16	Me	Me	7.0	4.8 (4.5–5.2)	25% at 180	17 (14–20)

^{a} The pK_a value of the conjugated acid of the pyrimidine nitrogen N1 estimated using

MarvinSketch. ^{b} Mean IC$_{50}$ for *T. brucei* AdoMetDC/prozyme at pH 7.2 determined using the

RapidFire–MS-based enzyme activity assay, in triplicate, with 95% confidence interval (CI)

shown in parentheses. ^{c} Mean IC$_{50}$ for human AdoMetDC at pH 7.2 determined in the

RapidFire–MS-based enzyme activity assay, in triplicate, with 95% CI shown in parentheses. ^{d}

Mean EC$_{50}$ as measured in the ATP–bioluminescence-based bloodstream form *T. brucei* Lister

427 cell viability assay, in triplicate, with 95% CI shown in parentheses. Percent inhibition at the

maximal tested concentration (in μM) is shown when maximum mean inhibition was <50%.

SAR studies: pyrimidine ring nitrogens and amino group. Next, compounds were

prepared to probe the function of the pyrimidine ring nitrogen atoms and C2-amino group (Table

2). Substitution of N1 with CH (**17** vs. **8**) led to complete loss of enzyme inhibitory activity

consistent with the hypothesized importance of protonated NH$^+$ base for binding. This activity

loss of 1-deaza analogs could not be rescued by moving the C2-amino group to the C6 position

(**18** and **19**). Conversely, replacement of N3 with CH led to only a 2–4-fold decrease in inhibitory activity (**20** and **21** compared with the respective parent compounds **7** and **8**). Interestingly, the pK_a(N1) for compounds with CH in place of N3 was predicted to increase by 2–3 units compared with the parent compounds. Thus the concentration of the N1-protonated species was expected to be >99% at pH 7.2, compared with only 55% or 20%, respectively, for the parent compounds, which was predicted to led to an increase in inhibitory activity. These data suggest that the positive gains of increased N1 protonation were offset by loss of other interactions with N3.

Table 2. SAR of pyrimidine ring nitrogens

Compound	X	Y	R^1	R^2	R^3	pK_a(N1)[a]	Tb IC$_{50}$,[b] μM	Hs IC$_{50}$,[c] μM	Tb427 EC$_{50}$,[d] μM
7	N	N	NH$_2$	Me	Cl	7.3	3.7 (3.3–4.1)	27% at 180	5.6 (4.5–7.1)
8	N	N	NH$_2$	H	Cl	6.6	13 (11–15)	>180	9.9 (7.7–13)
17	CH	N	NH$_2$	H	Cl	NA	>180	>180	96 (66–140)
18	CH	N	H	NH$_2$	Cl	NA	>180	>180	38 (31–47)
19	CH	N	Me	NH$_2$	Cl	NA	24% at 180	>180	13 (8.2–22)
20	N	CH	NH$_2$	Me	Cl	9.6	15 (13–18)	>180	2.2 (1.7–2.9)
21	N	CH	NH$_2$	H	Cl	9.4	29 (27–31)	>180	11 (9.5–12)
22	N	CNH$_2$	H	H	Cl	8.4	21% at 180	>180	18 (14–24)
23	N	N	H	Me	Cl	5.2	>180	>180	27 (22–33)
24	N	N	NHMe	Me	Cl	7.1	>63	>63	2.7 (2.4–3.1)
25	N	N	NMe$_2$	Me	Cl	7.0	>180	>180	14 (8.1–24)
26	N	N	NH$_2$	NH$_2$	Cl	6.4	48 (43–54)	>180	14 (12–17)
27	N	N	Me	NH$_2$	Br	6.4	24% at 180	>180	20 (17–24)

[a, b, c ,d] See footnotes for Table 1; NA, not applicable.

Deletion (**23**) or methylation (**24** and **25**) of the C2-amino group led to the loss of the enzyme inhibition. While the former decreased the pK_a(N1) to 5.2, the latter had little effect on the predicted pK_a for N1 protonation but introduced steric interactions preventing optimal
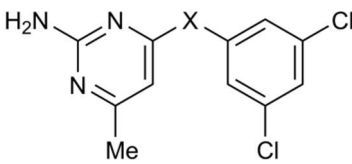
engagement of Glu266 (vide infra, Fig. 3B). Additionally, moving the C2-amino group to C3 in the background of a Me → H substitution at C6 led to further loss of inhibitory activity (**22** vs. **21**). Taken together, these data suggest the importance of the primary C2-amine and N1 for binding interactions, which was later supported by crystallographic data (vide infra) showing H-bonding and salt-bridge of a protonated pyrimidineamine to Glu266 (Fig. 3B).

Substituting an amino group for methyl at C6 (**26**) or swapping the C2-amino and C6-methyl groups (**27**; compare with the parent compound **44** in Table 4) resulted in lower $pK_a(N1)$ and a marked drop in the enzymatic inhibition. This is reflected in a better activity for **26** at pH 6.8 (5.8 µM against *Tb* AdoMetDC, see Table S1). Poorer activity of **27** can be rationalized by the loss of the C2-amino group essential for interaction with Glu266 (vide infra, Fig. 3B).

Notably, most compounds that showed poor enzyme inhibitory activity, with the exception of **17**, retained anti-trypanosomal activity, suggesting the presence of at least a partial off-target component in the mechanism of the cell growth inhibition.

SAR studies: linker variation. Having established the pyrimidine ring traits required for activity, we shifted our focus to understanding the role of the linker (Table 3).

Table 3. SAR of the linker
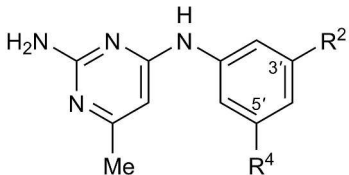
Compound	-X-	$pK_a(N1)^a$	*Tb* IC$_{50}$,^{b} µM	Hs IC$_{50}$,^{c} µM	*Tb*427 EC$_{50}$,^{d} µM
7	-NH-	7.3	3.7 (3.3–4.1)	27% at 180	5.6 (4.5–7.1)
28	-NMe-	7.2	81 (74–89)	>180	38 (34–43)
29	-S-	4.3	>180	>180	>25
30	-NH(CH$_2$)-	8.1	139 (130–150)	>180	11 (9.9–13)
31	-NH(CH$_2$)$_2$-	8.2	28 (25–32)	29% at 180	5.7 (1.6–21)

$^{a, b, c, d}$ See footnotes for Table 1.

Methylation of the linking amine (**28**) resulted in a sharp decrease in inhibitory activity in both enzyme and cell growth assays. The replacement of the amine with a thiol linker (**29**) eliminated enzyme inhibitory activity completely, presumably due to the effect on N1 acidity ($pK_a(N1) = 4.3$). Extension of the linker decreased potency to varying degrees. Addition of a single methylene (**30**) led to a 40-fold decrease in enzyme inhibition, while extension by two methylene units (**31**) decreased enzyme inhibition only by 8-fold.

SAR studies: aniline ring substitutions. We next focused our efforts on elucidating the role of the substituted aniline ring. Both the size and electronic nature of the substituents in the *meta* positions were probed first (Table 4). Replacement of one of the two chlorines in **7** with moderately sized or large functional groups (Br, CN, CF_3, Ph in **32–35**) was well tolerated and these analogs had *Tb*AdoMetDC IC_{50} values similar to the parent dichloro compound **7**. In contrast, pentafluorosulfanyl substitution led to 4-fold increase in the IC_{50} for *Tb*AdoMetDC inhibition (**36** and **37**). Since Br was a good substituent for Cl, we used 3-bromo analogs to probe the second *meta* positions of the aniline ring with alkyl and *O*-alkyl functionalities of varying length, including branched and unsaturated chains (**39–43**). All of these analogs showed *T. brucei* AdoMetDC inhibitory activity. The trifluoroethoxy of **40** conferred the highest potency of the tested substitutions, showing 3.8-fold lower IC_{50} than the similarly sized ethoxy of **39**. This underlines the importance of electronics in the terminal position of the substituent. Linear allyloxy and butoxy of **41** and **42**, respectively, performed 2.4-fold better than isobutoxy of **43** suggesting a preference for linear over branched substituents. Also, ethyl in **38** conferred activity similar to that of ethoxy in **39**, suggesting that the phenolic ether was dispensable.

Table 4. SAR of *meta* aniline ring substitutions

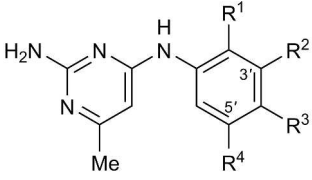| Compound	R^2	R^4	Tb IC$_{50}$,[b] µM	Hs IC$_{50}$,[c] µM	Tb427 EC$_{50}$,[d] µM
7	Cl	Cl	3.7 (3.3–4.1)	27% at 180	5.6 (4.5–7.1)
32	Br	Cl	2.2 (2.0–2.4)	33% at 180	4.7 (3.9–5.8)
33	CN	Cl	3.9 (3.2–4.8)	29% at 180	12 (10–14)
34	CF$_3$	Cl	3.9 (3.4–4.4)	39% at 180	13 (11–15)
35	Ph	Cl	3.3 (2.8–3.9)	30% at 63	4.5 (2.1–9.4)
36	SF$_5$	Cl	16 (14–18)	>180	13 (11–15)
37	SF$_5$	Br	8.7 (7.4–10)	>180	0.45 (0.32–0.62)
38	Et	Br	7.6 (5.7–10)	>180	5.5 (4.6–6.6)
39	OEt	Br	6.0 (5.2–6.9)	36% at 180	4.4 (4.2–4.7)
40	OCH$_2$CF$_3$	Br	1.6 (1.1–2.4)	44	4.2 (3.6–4.8)
41	OCH$_2$CHCH$_2$	Br	4.5 (4.1–4.9)	28% at 180	4.4 (3.7–5.3)
42	OBu	Br	4.5 (4.0–5.1)	>180	1.9 (1.7–2.1)
43	OCH$_2$^{i}Pr	Br	11 (9.5–12)	>180	4.4 (3.5–5.5)
44	Br	Br	1.9 (1.7–2.1)	31% at 180	4.8 (4.1–5.6)
45	SO$_2$Me	SO$_2$Me	1.5 (1.3–1.7)	39% at 180	>100
46	CF$_3$	CF$_3$	11 (9.8–12)	>180	14 (11–17)
47	OMe	OMe	17 (14–20)	21% at 180	41 (33–51)
48	CO$_2$H	CO$_2$H	>180	>180	>100
49	CO$_2$Me	CO$_2$Me	40% at 180	>180	42 (22–78)
50	Ph	Ph	>180	>180	1.5 (1.3–1.6)
51	*N*-(3,5-Cl$_2$Ph)-acetamide	*N*-(3,5-Cl$_2$Ph)-acetamide	>180	>180	2.0 (1.2–3.7)
52	Me	Me	141 (119–167)	>180	19 (17–22)
53	^{t}Bu	^{t}Bu	>63	>63	4.1 (4.1–4.5)
54	SF$_5$	H	23% at 180	>180	14 (11–17)
55	Cl	H	35% at 180	>180	42 (34–52)
56	Br	H	41% at 180	>180	22 (19–26)
57	F	H	>180	>180	>25
58	SMe	H	149 (122–181)	23% at 180	>25
59	H	H	>180	>180	>25
60	F	F	180 (160–201)	>180	70 (61–80)
61	F	Cl	32 (13–82)	>180	17 (15–20)

All compounds have pK_a(N1)[a] of 7.3. [a, b, c, d] See footnotes for Table 1.

When both chlorines were simultaneously replaced with either bromines (**44**) or methylsulfonyls (**45**), inhibitor potency on the enzyme was improved by 2-fold (although **45** had no antitrypanosomal activity, presumably due to impaired cell uptake). Conversely, other moderately sized nonpolar and polar (Me, *t*-Bu, CF$_3$, OMe, CO$_2$H, CO$_2$Me) or larger aryl (Ph and *N*-(3,5-(di-Cl)-Ph)-acetamide) substituents in both *meta* positions led to reduced (**46** and **47**) or nearly absent (**48–53**) enzyme inhibitory activity. Removal of one or both *meta*-substituents (**54-59**) or replacement with a smaller fluorine-substituent (**60**, **61**) substantially reduced (**54-56**, **58**, **60**, **61**) or eliminated (**57**, **59**) enzyme inhibitory activity.

The correlation between enzyme and cell growth inhibition was dependent on the aniline-ring substitution pattern. Both enzyme and cell-based activity correlated reasonably for analogs **32-44**, **46-49**, **52**, **57-61**, whereas enzyme-inactive compounds **50**, **51**, **53** retained substantial antitrypanosomal activity indicating off-target activity. The very weak AdoMeDC inhibitors **54-56** did retain some, albeit reduced cellular activity indicating a partial off-target activity or increased cellular uptake/accumulation.

Having established the effects of *meta*-substitution, we looked at SAR related to substitution patterns that include *ortho* and *para* positions (Table 5).

Table 5. SAR of *ortho*- and *para*-aniline ring substitutions

Compound	R^1	R^2	R^3	R^4	*Tb* IC$_{50}$,[b] µM	*Hs* IC$_{50}$,[c] µM	*Tb*427 EC$_{50}$,[d] µM
7	H	Cl	H	Cl	3.7 (3.3–4.1)	27% at 180	5.6 (4.5–7.1)
62	H	Cl	F	Cl	1.5 (1.4–1.8)	160 (135–191)	4.8 (3.3–7)
63	H	Br	F	Br	1.6 (1.3–1.8)	43% at 180	4.6 (3.6–5.9)
64	H	Cl	Cl	Cl	11 (8.8–13)	>63	4.5 (3.4–5.9)
65	H	Cl	Me	Cl	20 (17–24)	>63	4.4 (4.2–4.8)
66	H	Cl	OPh	Cl	38% at 180	>180	1.1 (0.97–1.3)
67	H	Cl	OH	Cl	33% at 180	>180	13 (10–16)
68	H	Cl	OCHF$_2$	Cl	>63	>63	4.5 (3.7–5.4)
69	H	Cl	NMe$_2$	Cl	>180	>180	5.8 (4.2–7.9)
70	H	Cl	*N*-morpholino	Cl	>180	>180	18 (14–24)
71	H	Cl	*N*-piperidino	Cl	>180	>180	2.1 (1.3–3.2)
72	OH	Cl	H	Cl	37 (29–46)	>180	26% at 100
73	F	Cl	F	Cl	2.2 (2.0–2.6)	>63	10 (8.5–12)
74	Cl	H	H	Cl	115 (89–150)	>180	23% at 25
75	Cl	Cl	H	H	137 (95–198)	>180	27% at 25
76	Cl	H	Cl	H	>180	>180	28% at 25
77	Me	H	H	H	>180	>180	>25
78	SMe	H	H	H	>180	>180	>25
79	Br	H	H	H	>180	>180	>25
80	Me	Cl	H	H	>180	>180	29% at 25
81	Me	H	H	Cl	>180	>180	28% at 25
82	Me	H	Cl	H	>180	>180	>25
83	F	H	Br	H	>180	>180	25% at 25
84	Cl	H	H	CF$_3$	199 (164–240)	>180	28% at 25
85	H	H	Cl	H	>180	>180	28% at 25
86	H	H	Et	H	>180	>180	19 (17–22)
87	H	H	*i*Pr	H	>180	>180	11 (8.5–15)
88	H	H	CF$_3$	H	>180	>180	15 (13–17)
89	H	H	3,5-Cl$_2$Ph	H	>180	>180	1.0 (0.88–1.2)
90	H	F	F	H	33% at 180	>180	25% at 25

All compounds have pK_a(N1)[a] of 7.3 except **67** (pK_a(N1)= 7.0); **72** (pK_a(N1)= 7.1); **73**, **74**,

and **83** (pK_a(N1)= 7.2). [a, b, c, d] See footnotes for Table 1.

Introduction of a fluorine into the *para* position led to up to 2-fold enhancement in potency

towards *Tb*AdoMetDC (**62**, **63** vs. **7**, **44**), whereas chlorine and methyl-substitution (**64**, **65**)

reduced activity 3 to 6-fold vs. comparator **7**. All other *para*-substituents that were explored,

irrespective of size or electronic nature, led to a complete loss of inhibitory activity towards the

enzyme. Retrospectively, this SAR is in agreement with the co-crystal structure data, which

indicates a size-restriction in the AdoMetDC binding pocket along the *para*-position vector (vide

infra, Fig. 3B). The *ortho* position tolerated addition of a fluoro (**73**), but substitution with OH

(**72**) resulted in ten-fold reduced inhibitory activity vs. **7**. Addition of a Cl, Br, Me, or SMe

substituent in the *ortho*-position of the inactive unsubstituted phenyl analog **59** or very weakly

active mono *meta*-chloro or bromo analogs **55** or **56** was ineffective at introducing any activity

for compounds **74-84** (some additional inactive compounds are shown in Table S2).

In this series, there was a reasonable correlation between the activity on the enzyme and

cellular activity for compounds without *para*-substituents or with *para*-halogens (**62-64**, **72-85**,

90). However, this correlation breaks down for every other *para*-substituted compounds tested

(**65-71**, **86-89**). Notably, enzyme inactive *para*-substituted analogs **66-71** and **86-89** retained

substantial antitrypanosomal activity, with EC_{50} values between 1 and 20 µM.

The data so far suggested that *meta*-positioning of substituents on the aniline ring was

crucial for activity and minimizing off-target antitrypanosomal activity. Minimally, one of the

two *meta*-positions requires substitution with a chlorine or bromine, whereas the other *meta*-

position needs to be substituted but has more flexibility such that halogens, cyano, CF_3, Et,

alkylethers, and Ph can be accommodated. However, while these modifications were tolerated,

none resulted in a compound with substantially increased potency over the parent compound.

Since we discovered that phenyl in one of the two *meta*-positions yielded an active compound

(**35**, see Table 4), we prepared a number of substituted phenyl, heteroaromatic, and fused-ring analogs, aiming to further tune the inhibitory activity and off-target antitrypanosomal activity (Table 6).

Compared to the parent *meta*-phenyl substituted biaryl analog **35**, 4-FPh and 4-ClPh substituted biaryl analogs **91** and **92** were about 2 to 3-fold more potent in the enzyme and cell-based assays, whereas 4-OMe, 4-Me, and 4-CF$_3$ substitution delivered roughly equipotent compounds in both assays (**93**–**95**). A 2-fold loss of enzyme inhibition was observed for the 4-CNPh analog (**96**), but this was accompanied by an increase in cellular activity (~5-fold). Moving to 4-Ac (**97**), 4-OH (**98**), and 4-NMe$_2$ (**100**) substituents, enzyme inhibition dropped off markedly but cell-based inhibition remained at single-digit micromolar EC$_{50}$ levels, indicating off-target activity. Similarly, moving chlorine to the 2- or 3-position (**101**, **102**), adding an extra Cl or CF$_3$ to the 3-position (**103**–**105**), or 3,5-(CF$_3$)$_2$-substitution (**106**) also abolished enzyme inhibition while retaining the off-target cell-based activity.

Biaryls (4-PhPh, **99**), polycyclic aryls (naphthyl **107**, phenanthrenyl **108**), benzofused heteroaryls (**110**, **112**, **114**), or 5-membered heteroaromatics (5-thiazolyl **115**, *N*-Me-4-pyrazolyl **116**) were largely incompatible with enzyme inhibition but retained potent off-target cell activity. Enzyme and cell activity tracked better for benzodioxolyl (**109**), furanyl (**111**), thiophenyl (**113**), and pyrimidinyl (**117**) substituents, with the former two (**109**, **111**) active in the low micromolar range, and the latter two (**113**, **117**) largely devoid of activity in both assays. Finally, we prepared and tested compound **118** that combined 4-fluorophenyl and ethyl *meta*-substitutions. Compared to the corresponding 3-(4-FPh)-5-Cl analog **91**, the similar activity of **118** indicates that *meta*-Cl can be exchanged for *meta*-Et without affecting enzyme or cell-based potency.

1
2
3
4
5
6
7
8
9
10
11
12
13
14
15

Table 6. SAR of *meta*-aryl aniline ring substitutions
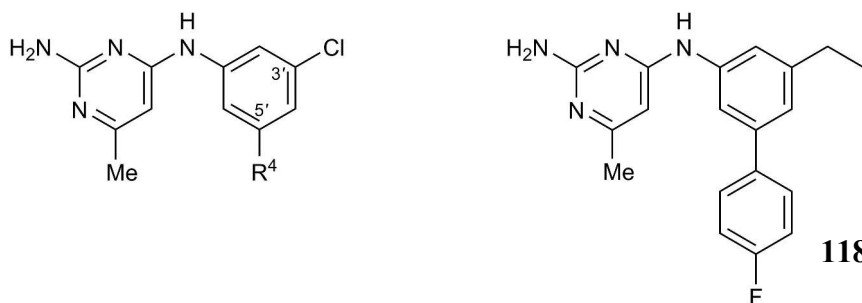
Compound	R^4	*Tb* IC$_{50}$,[b] µM	*Hs* IC$_{50}$,[c] µM	*Tb*427 EC$_{50}$,[d] µM
35	Ph	3.3 (2.8–3.9)	30% at 63	4.5 (2.1–9.4)
91	4-FPh	1.1 (0.95–1.2)	>21	1.6 (0.94–2.8)
92	4-ClPh	1.7 (1.6–2.0)	>63	2.2 (1.8–2.7)
93	4-MeOPh	2.3 (2.1–2.6)	>180	4.5 (3.1–6.6)
94	4-MePh	4.6 (4.0–5.3)	>63	4.3 (3.3–5.7)
95	4-CF$_3$Ph	4.7 (3.9–5.7)	>21	2.0 (1.4–3)
96	4-CNPh	7.6 (3.2–18)	>7	1.0 (0.96–1.1)
97	4-AcPh	28% at 21	>21	6.7 (4.1–11)
98	4-HOPh	143 (115–178)	>180	9.7 (7.5–13)
99	4-PhPh	167 (150–190)	>180	0.91 (0.82–1)
100	4-NMe$_2$Ph	34% at 180	>180	5.0 (4.2–6)
101	2-ClPh	26 (22–33)	>180	8.5 (7.6–9.5)
102	3-ClPh	81 (57–114)	>180	1.9 (1.6–2.3)
103	3,4-(Cl)$_2$Ph	102 (82–125)	>180	2.9 (1.3–3.6)
104	3-Cl-4-FPh	157 (95–260)	>180	3.2 (2.8–3.7)
105	3-CF$_3$-4-ClPh	53 (46–61)	>180	1.5 (1–2.2)
106	3,5-(CF$_3$)$_2$Ph	28 (25–31)	>180	0.53 (0.47–0.59)
107	2-naphthyl	57 (51–64)	>180	1.7 (1.4–2)
108	9-phenanthrenyl	>180	>180	1.8 (1.5–2.1)
109	5-benzo-1,3-dioxolyl	6.2 (4.6–8.3)	>21	2.3 (1.6–3.2)
110	5-benzofurazanyl	27 (21–35)	>180	0.57 (0.13–2.5)
111	3-furanyl	7.4 (6.2–8.7)	30% at 180	7.1 (5.7–8.8)
112	2-benzofuranyl	23% at 63	>63	1.4 (1.4–1.5)
113	3-thiopheneyl	26 (22–32)	30% at 180	29 (23–35)
114	2-benzothiopheneyl	41 (36–46)	>180	1.6 (1.5–1.8)
115	5-thiazolyl	42% at 21	>21	3.6 (3.1–4.1)
116	*N*-Me-4-pyrazolyl	164 (132–203)	>180	6.7 (4.7–9.6)
117	5-pyrimidinyl	>180	>180	58 (33–100)
118		2.7 (2.2–3.4)	>180	1.3 (1.1–1.5)

All compounds have pK_a(N1)[a] of 7.3. [a, b, c, d] See footnotes for Table 1.

56
57
58
59
60

Crystal structure of *Tb*AdoMetDC/prozyme in complex with a pyrimidineamine analog

reveals binding interactions. To assist in rational design of pyrimidineamine analogs with

improved binding properties, we solved the crystal structure of the *Tb*AdoMetDC/prozyme

complex co-crystallized with **44**. Compound **44** was selected for co-crystallization on the basis of

its potency and solubility in aqueous solutions. Additionally, the presence of two bromines

facilitated location of the bound compound in the complex, and the anomalous diffraction data

collected at the Br K-edge were instrumental in determining the correct orientation of this quasi-

symmetrical molecule in the binding pocket (See Experimental methods). The structure was

solved by molecular replacement using our previously determined *Tb*AdoMetDC/prozyme

heterodimeric structure (Protein Data Bank (PDB) identifier 5TVM)[21] as a search model, and

refined to 3.0 Å resolution with R_{work}/R_{free} = 20.0/25.3%. Overall, the structure was similar to the

unliganded active heterodimer (RMSD of 0.28 Å between current structure and 5TVM as

determined by *TM-align*[34] for 636 equivalent C_α atoms).

A single molecule of **44** was found in the catalytic site of the *Tb*AdoMetDC in the

heterodimer of *Tb*AdoMetDC/prozyme, positioned 3.9 Å from the catalytic pyruvate (Figure

3A). This binding mode is consistent with biochemically demonstrated competitive mode of

inhibition (see Figure 2B). The binding interactions observed between **44** and the enzyme also

explain much of the above described SAR for the series. The requirement for N1 to be

protonated and for C2 to have a primary amine is explained by the finding that both groups are

within hydrogen-bonding distance of the side-chain carboxyl oxygens of Glu266 in the binding

pocket. It is thus reasonable to assume that a protonated pyrimidineamine participates in

favorable bidentate H-bonding and salt-bridge interactions (Figure 3B).

Additional binding energy is also likely contributed by π–π stacking interactions between

the pyrimidine ring and Phe28, and between aniline ring and Tyr243. The proximity of the

catalytic Cys100 to the aniline ring of **44** (3.2 Å between SH and C4' of the ring) is suggestive of

the aromatic–thiol interaction (Figure 3B), though the angle of the interaction is not ideal as

determined by previously described interactions of this type.[35, 36] Finally, an H-bonding

interaction[37] between the partially negative lateral end of one of the aniline ring *meta*-bromines

and Ser249 hydroxyl group is also potentially present, and may contribute to the binding energy

(Figure 3B).

Importantly, the structure of *Tb*AdoMetDC co-crystallized with **44** revealed that the 3'- and

5'-substituents on the aniline ring projected into two distinct pockets designated *a* and *b* (Figure

3B). Building on the structural data and the observations reported in Tables 4–6, we hypothesize

that of the two pockets, only pocket *a* could accommodate a phenyl-sized substitution at the

meta-position of the aniline ring. Conversely, the shape and depth of pocket *b* suggested that it

would be accessible to linear, flexible substituents (for example, alkyls and alkyl ethers **38-43** in

Table 4). The fact that **118**, functionalized with *p*-fluorophenyl at one *meta*-position and ethyl at

the other, inhibited the enzyme with good potency ($IC_{50} = 2.7$ μM, see Table 6) suggests that

both pockets can be accessed simultaneously in the context of a single compound. Additionally,

our structure suggested that *para*-substituents larger than F, Cl, or Me would be inaccessible as

confirmed by the enzyme inhibition data in Table 5 (**66-71**).

Structural basis for parasite–host selectivity. *Hs*AdoMetDC (PDB identifier 3DZ7)[38] was

aligned to the *Tb*AdoMetDC bound to **44** to provide insight into the structural basis for

selectivity of this and other pyrimidineamines for *T. brucei* AdoMetDC compared with the

human enzyme (Figure 4). The catalytic sites are mostly conserved between the two species, and

their geometries are similar. One residue at the lid of the pocket, however, differs between them. This residue (His5 in human AdoMetDC and Arg26 in *T. brucei* AdoMetDC) is positioned differently in the two structures. His5 in human AdoMetDC is within 3.2 Å of **44** in the overlaid enzyme, and may function to restrict the ligand-binding site compared with the *T. brucei* structure (Figure 4). The analogous position in *T. brucei* AdoMetDC (Arg26) was not well resolved in the electron density maps of the structure reported herein; however, it was observed in previous structures (PDB depositions 5TVF and 5TVM) where it was positioned away from the opening of the binding pocket (Figure 4).

Additionally, the substitution of Cys49 in the human structure for Ala67 in *T. brucei* AdoMetDC restricts the size of the human pocket *a* relative to *T. brucei* (Figure 4). This size restriction would be expected to provide additional selectivity for analogs that have larger substituents in pocket *a*, such as the *p*-fluorophenyl of **91** and **118**.

On-target mechanism-of-action studies. As was noted above, the correlation between the enzyme and cell-growth inhibition was weak. This suggested that trypanocidal effect was at least in part due to off-target mechanism of action. Thus, we sought to identify whether the pyrimidineamines were inhibiting AdoMetDC in *T. brucei* cells. We previously reported that the levels of prozyme protein markedly increased when AdoMetDC activity in *T. brucei* cells was reduced by either genetic knockdown of AdoMetDC or by chemical inhibition.[16, 39] We exploited this feedback loop to evaluate whether hit compounds identified in the HTS were affecting the parasite cell growth through intracellular AdoMetDC inhibition.[22] Here, we compared prozyme protein levels in cells treated for 24 h with representative pyrimidineamine analogs that 1) inhibited both *T. brucei* cell growth and AdoMetDC (**7** and **8**), 2) inhibited only *T. brucei* growth (**23** and **13**), or 3) were inactive in both assays (**29**). Only compounds that were active on both

the enzyme and cells induced prozyme above the vehicle-only control levels (Figure 5). These results show that the pyrimidineamines with *Tb*AdoMetDC inhibitory activity on the purified enzyme also block AdoMetDC activity in *T. brucei* cells. However, these results also confirm that there was a substantial off-target component to pyrimidineamine-induced cell growth inhibition, as **23** and **13**, which did not inhibit *Tb*AdoMetDC — either in the purified-enzyme assay or in the cell (as evident from vehicle-only levels of the prozyme protein) — inhibited cell growth with low-micromolar potencies (Figure 5).

Discussion and Conclusions

The number of cases of HAT has decreased 10-fold since the beginning of the 21st century owing to proactive surveillance and control measures set in place in endemic countries.[3] Yet the disease has a history of resurgence following years of a downward trend.[3] Sustainability of HAT elimination relies in part on the availability of patient-friendly treatment options.[3] Neither melarsoprol nor eflornithine, alone or as a part of NECT, are ideal due to high toxicity of the former and high price and requirement for multiple intravenous infusions of the latter.[2, 10] The potential for eflornithine resistance to emerge is another negative factor.[40] Thus, new safe anti-trypanosomal drugs with CNS-stage efficacy are needed.

We identified and characterized a pyrimidineamine series as a new class of reversible, competitive inhibitors of *T. brucei* AdoMetDC. This series has a number of positive attributes, including species-selective inhibition of the *T. brucei* AdoMetDC compared with the human enzyme and antitrypanosomal activity against *T. brucei* in whole-cell assays. Importantly, the series is predicted to have good brain penetration on the basis of the monolayer permeability assay performed on the parent compound. Thus, the pyrimidineamines have the potential to be used for treatment of both early-stage and late-stage HAT. Herein, we have established the

preliminary SAR within the series and have solved the crystal structure of one analog bound to

T. brucei AdoMetDC, providing insight for future lead optimization of the series.

While the pyrimidineamines look to be a promising series for further optimization, three key

issues were identified that would need to be addressed in future chemistry programs. Firstly,

while the pyrimidineamines did show activity against both the enzyme and the parasite, the

correlation between these activities was poor. On-target activity was present as evident from the

finding that prozyme was upregulated in cells treated with compounds that inhibited AdoMetDC.

In addition, good correlation between enzyme inhibition and anti-parasite activity was observed

for most active analogs with two *meta*-substituents in the aniline ring, with at least one

substituent being Cl or Br. If the second *meta*-position is a phenyl-ring substituted in the 4-

position with F, Cl, OMe, Me, or CF_3, good activity in both assays was observed. However, there

was also clear evidence for an off-target activity, as a substantial fraction of pyrimidineamines

that had lost *Tb*AdoMetDC inhibitory activity elicited cell growth inhibition in the low-

micromolar range. Off-target activity was especially noticeable for *para*-substituted aniline rings

(Table 5) and bis-*meta*-substituted aniline rings with on *meta*-position occupied by 2-, 3-, 2,3- or

other specifically substituted aryls, biaryls, polycyclic aryls and heteroaryls (Table 6). Secondly,

despite synthesis of a number of analogs of the original parent compound, we were unable to

substantially improve compound potency below the low-micromolar level. This issue may also

relate to the off-target activity, and thus identification of more potent analogs may lead to

reduced off-target activity as the on-target component improves. As the analogs described herein

had been synthesized prior to obtaining the crystal structure with an inhibitor bound, there

remains room for a structure-based lead optimization program to facilitate the identification of

more potent, on-target compounds. Lastly, **7** showed poor metabolic stability; however, this

liability was not the focus of the current chemistry program and remains to be addressed during further optimization of the series.

A notable feature of pyrimidineamines is the finding that inhibitor binding to *Tb*AdoMetDC is pH-dependent in the relevant physiological range (pH 6.8–7.7). This dependence has its basis in the pK_a of N1 in the pyrimidine ring, which is predicted to be 7.3 in the parent compound **7**. Within the series, modifying the ring substituents to lower the pK_a(N1) (<6) led to reduced inhibitory activity at physiological pH, while optimizing the ring electronics to yield a higher pK_a(N1) (>9) reduced the pH dependence of binding. The crystal structure of *Tb*AdoMetDC bound to **44** revealed that N1 forms a salt bridge with Glu266, explaining the requirement for protonation of N1 for inhibitor binding. While we were able to identify compounds with higher pK_a, this was achieved through removal of N3 (**20** and **21**), which led to a loss of the possible interaction between N3 and main-chain carbonyl of Cys246 (3.5 Å away, see Figure 3B). Thus we did not accomplish the goal of improved binding affinity by this strategy. One potential direction for future optimization of this series will be to identify compounds that retain full charge at N1 at physiological pH, without compromising other binding interactions.

In addition to the protonation state of N1, we identified a number of other features of the pharmacophore that were required for *Tb*AdoMetDC inhibition. A primary amine is required at C2, and it is involved in an H-bond with the Glu266 carboxyl group. The amine linker could not be modified as there was a loss of potency when the linker was methylated (**28**), extended by one or two methylene links (**30** and **31**), or replaced with sulfur (**29**). The amine linker does not make any clear interactions with the protein, so its importance may relate to geometry and steric considerations. For sulfur-linked analog **29**, the decreased pKa at N1 (4.3) could explain the loss of enzyme inhibition. Finally, both pyrimidine and aniline rings are required, and these form

stabilizing π–π stacking interactions with the two aromatic residues, Phe28 and Tyr243, on opposite sides of the catalytic site.

The aniline ring is the most buried part of the ligand. SAR and the crystal structure indicate that substituents in both of the *meta*-positions are required for good binding. We identified both steric and electronic requirements to the *meta*-substitutions. At least one of the *meta*-positions can include an alkyl, alkyloxy, halide, or 4-substituted phenyl ring; whereas the second position is best occupied by Cl, or Br. Notably, both an alkyl (ethyl) and a 4-substituted phenyl could be accommodated at the same time as indicated by anti-*Tb*AdoMetDC activity of **118**. A hydrogen bond between Ser249 γ-hydroxyl and a partially negative acceptor in a *meta* position, such as halide or alkoxy may contribute to the binding energy and explain the finding.[37] The next steps, informed by the co-crystal structure data, will involve a much more in depth combinatorial exploration of both *meta*-positions in such a manner as to ideally occupy both *a* and *b* pockets as well as maximize π–π stacking interactions.

All active analogs were strongly selective for *T. brucei* AdoMetDC over the human enzyme. The selectivity ratio (HsIC$_{50}$/TbIC$_{50}$) was at least 27 (**40**) and in many cases exceeded 100 (e.g., **44** and **62**). Yet, the structural basis for species selectivity was not immediately obvious given very similar geometries and residue composition of the catalytic sites in the two species. Specifically, the human site has Phe7 and Phe223 in the positions analogous to *T. brucei* Phe28 and Tyr243, which could provide π–π stacking interactions with a compound (see Figure 4). Also, Glu247 in the human enzyme closely aligns with *T. brucei* Glu266, and could potentially also form H-bonding and salt-bridge interactions with pyrimidineamine part of an inhibitor. One possible hypothesis suggested by our co-crystal structure is that His5 in the human AdoMetDC sterically limits access to the binding site, excluding certain classes of inhibitors and thus may be

responsible for the observed species selectivity of the pyrimidineamines. In *T. brucei*, the equivalent position is occupied by an Arg residue with a more labile side chain (see Figure 4). Notably, all 13 classes of validated active hits from our HTS campaign were also selective inhibitors of the *T. brucei* enzyme,[22] suggesting this may be a general principle of parasite–host selectivity. In contrast, a number of compounds that have greater binding affinity for the human enzyme have also been described, such as methylglyoxal bis(guanylhydrazone), or MGBG,[41] and CGP 40215,[42] so evidently this mechanism does not limit general access to the active site. An additional possible origin for species selectivity can be inferred from the allosteric mechanism of *T. brucei* AdoMetDC activation: its N-terminal residues form an autoinhibitory lid blocking the active site in the monomer that is displaced from the active site upon binding to prozyme.[21] Conversely, the N-terminus of the human enzyme is 21 residues shorter than that of the *T. brucei* enzyme, and it has not been observed to bind in the active site in any of the published X-ray crystal structures.[38, 43-45] However, these data do not rule out the possibility that these residues undergo dynamic transitions during catalysis or ligand binding. Thus, potentially selectivity could arise if the N-terminal residues of the human enzyme compete for ligand binding. In this scenario, *T. brucei* selective inhibitors would be unable to effectively compete with the N-terminal residue lid, whereas human selective inhibitors and substrate would be effective competitors. Finally, we note that pocket *a* in human AdoMetDC is smaller than in the *T. brucei* enzyme, and this difference will enhance selectivity for compounds that fully occupy this pocket (e.g., **91**), though this difference is unlikely to explain the selectivity of compounds with smaller substitutions in pocket *a* (e.g. **44**).

The work described herein has led to the discovery of pyrimidineamines with low-micromolar activity against both *T. brucei* AdoMetDC and the parasite. Through a combination

of medicinal chemistry and protein crystallography, we have defined the key components of the

pharmacophore that are required for *Tb*AdoMetDC inhibitory activity. If this series is to advance

to lead optimization, future work will need to focus on identifying more potent compounds. Two

pockets were discovered in the crystal structure that were not fully exploited in the current work.

Pocket *a* is larger of the two and is lined with both polar (Glu85 and Pvl86) and nonpolar (Ile65,

Ala67, Leu83, and Ile103) side chains (see Figure 3B). The *p*-substituted phenyl analogs such as

91 provided for good size complementarity with the available pocket but the crystal structure and

activity data suggest that more polar substituents that could engage in H-bonding interactions

with Glu85 and backbone carbonyls in the pocket might provide better binding energy (see Table

6 and Figure 3B). Alternatively, a nucleophilic group (e.g, aminooxy) might allow formation of a

Schiff base with the prosthetic pyruvoyl group, transforming pyrimidineamines into mechanism-

based inhibitors, as described for substrate analogs.[46] Pocket *b* also has substantial polar

character with several opportunities for H-bonding interactions presented by side chains of

Glu32, Ser273, Ser249, and His262 (see Figure 3B). Current ring substituents did not fully

exploit these opportunities and thus further series development should focus on optimizing these

potential polar interactions at the *meta*-positions of the aniline ring. The search of the suitable

substituents can be aided by computational protein–ligand docking through virtual screening of

meta-position analogs. Iterative co-crystallization with new analogs will aid development.

Experimental Section

Chemistry. *General Procedures.* Unless otherwise specified, all commercially available

reagents were used as received. All reactions using dried solvents were carried out under an

atmosphere of argon in flame-dried glassware with magnetic stirring. Dry solvent was dispensed

from a solvent purification system that passes solvent through two columns of dry neutral

alumina. Silica gel chromatographic purifications were performed by flash chromatography with

silica gel (Sigma, grade 62, 60-200 mesh) packed in glass columns; the eluting solvent was

determined by thin layer chromatography (TLC). Analytical TLC was performed on glass plates

coated with 0.25 mm silica gel using UV for visualization. Melting points are uncorrected.

Routine ^{1}H and proton-decoupled ^{13}C NMR spectra were obtained on a Bruker 400 MHz NMR

spectrometer. Chemical shifts (δ) are reported in parts per million (ppm) from low to high field

relative to residual solvent. Multiplicities are given as: s (singlet), d (doublet), t (triplet), q

(quartet), dd (doublet of doublets), m (multiplet). All synthetic compounds exhibited >95%

purity as determined by LC-MS analysis performed on an Agilent 1100 HPLC system using an

Eclipse XDB-C18 column (4.6 × 150 mm, 5 μm; Agilent) that was coupled to an Agilent

G1956A (or 6120) ESI mass spectrometer run in the positive mode with a scan range of 100 to

800 (or 1000) m/z. Liquid chromatography was carried out at a flow rate of 0.5 mL/min at 30 °C

with a 5 μL injection volume, using the gradient elution with aqueous acetonitrile containing

0.1% formic acid: 20–50% over 10 min followed by 50–90% for the next 10 min. All tested

purchased compounds were verified to be >95% pure using the method described above with the

following modifications: Agilent Infinity II HPLC system coupled to an Agilent 6120 ESI mass

spectrometer was used; the range was from 100 to 1000 m/z; flow rate was 0.8 mL/min; and

gradient elution was done with aqueous acetonitrile containing 0.1% trifluoroacetic acid: 10-

100% over 7 min followed by 100% for the next 8 min.

General Procedure A (for the synthesis of compounds 13, 14, 23-25, 27, 28, 38-43, 46-48, 52, 55, 60, 69-71). To a stirred solution of chloropyrimidine **2a,d,e,h** or **3d-f,h** (1 equiv.) and substituted aniline (1 equiv.) in EtOH (4 mL/mmol) was added conc. HCl (0.1 mL/mmol). The solution was then heated to reflux for 18 h. After cooling to rt, the volatiles were concentrated *in vacuo*. The residual oil was partitioned between EtOAc (4 mL/mmol) and 10% aq. NaOH (4 mL/mmol). The layers were separated and the aqueous layer was extracted with EtOAc (3 ×; 4 mL/mmol). The combined organic layers were dried (Na_2SO_4) and concentrated. The resulting residue was purified by flash chromatography.

General Procedure B (for the synthesis of compounds 18-20, 22). The appropriate chloropyridine **3a,c,i,j** (1 equiv.) was dissolved in *n*-BuOH (1.23 mL/mmol chloropyridine) in a microwave vial before 3,5-dichloroaniline (1.5 equiv.) was added followed by concentrated HCl (0.154 mL/mmol chloropyridine). The vial was sealed and the solution was heated in the microwave at 185 °C for 4 h before being cooled to rt and diluted with 30 mL of EtOAc (4.6 mL/mmol chloropyridine). 10% Aq. NaOH (4.6 mL/mmol chloropyridine) was added, the layers were separated and the aqueous layer was extracted with EtOAc (3 ×; 2.3 mL/mmol chloropyridine). The organic layers were combined, dried (Na_2SO_4) and concentrated *in vacuo*. The resulting residue was purified by flash chromatography.

General Procedure C (for the synthesis of compounds 9, 10, 15, 16, 26, 32-34, 36, 37, 44, 45, 53, 54, 61-68, 72, 73, 89). The appropriate aniline (1 equiv.) and chloropyrimidine **2a-c,f-h** or **3g** (1 equiv.) were dissolved in EtOH (1.03 mL/ mmol) containing concentrated HCl (0.129 mL/mmol) in a microwave vial. The vial was sealed and the solution was heated in the microwave at 140 °C for 1.5 hours before being cooled to rt and diluted with 10 mL of EtOAc

(5.15 mL/mmol). 10% Aq. NaOH (5.15 mL/mmol) was added, the layers were separated and the

aqueous layer was extracted with EtOAc (3 ×; 5.15 mL/mmol). The organic layers were

combined, dried (Na_2SO_4) and concentrated *in vacuo*. The resulting residue was purified by flash

chromatography.

General Procedure D (for the synthesis of compounds 11, 50, 91-109, 116-118). To a

solution of sodium carbonate (3 equiv.) in water (1 mL/mmol carbonate) and DME (3.33

mL/mmol carbonate) was added arylchloride **7** or **13** or arylbromide **32** or **38** (1 equiv.),

phenylboronic acid (1.1 equiv.) (note: 2.2 equiv. are used for bis-arylation) and PPh_3 (0.244

equiv.). The solution was evacuated and backfilled with Ar 5× before $Pd(OAc)_2$ (0.122 equiv.)

was added. The solution was again evacuated and backfilled with Ar 5× before being heated to

90 °C for 18 h. The solution was cooled to rt and filtered through Celite. The filtrate was diluted

with EtOAc (29 mL/mmol arylhalide) and the solution was washed with 10% aq. NaOH

followed by brine. The organic layer was dried (Na_2SO_4), filtered and concentrated *in vacuo* to

afford a residue that was purified by flash chromatography.

General Procedure E (for the synthesis of compounds 110-115). To a solution of sodium

triphosphate (7.48 equiv.) in water:dioxane (1:4; 13 mL/mmol **32**) was added bromopyrimidine

32 (1 equiv.), and PPh_3 (0.3 equiv.). The solution was evacuated and backfilled with Ar 5×

before the appropriate heteroaryl boronic acid MIDA ester (1.19 equiv.) was added. The solution

was again evacuated and backfilled with Ar 5× and $Pd(OAc)_2$ (0.145 equiv.) was added. The

solution was again evacuated and backfilled with Ar 5× before being heated to 90 °C for 18 h.

The solution was cooled to rt and filtered through Celite. The filtrate was diluted with EtOAc (48

mL/mmol **32**) and the solution was washed with 10% aq. NaOH followed by brine. The organic

layer was dried (Na$_2$SO$_4$), filtered and concentrated *in vacuo* to afford a residue that was purified by flash chromatography.

***N*^{2}-(3,5-Dichlorophenyl)pyridine-2,4-diamine (18)** According to General Procedure B, 2-chloropyridin-4-amine (1.0 g, 7.76 mmol) and 3,5-dichloroaniline (2.50 g, 15.5 mmol) yielded compound **18** as an off-white solid (0.75 g, 39%); mp >250 °C. ^{1}H NMR (400 MHz, Methanol-*d*$_4$) δ 7.95 (s, 1H), 7.73 (d, *J* = 5.5 Hz, 1H), 7.06 (d, *J* = 5.5 Hz, 1H), 6.97 (d, *J* = 1.8 Hz, 2H), 6.93 (t, *J* = 1.8 Hz, 1H). ^{13}C NMR (101 MHz, CD$_3$OD) δ 144.6, 138.6, 136.3, 135.5, 135.2, 121.6, 120.3, 116.0, 111.9. LC/MS (ESI) calcd for C$_{11}$H$_{10}$Cl$_2$N$_3$ (M + H)$^+$ 254.0, found 254.0.

***N*^{2}-(3,5-Dichlorophenyl)-6-methylpyridine-2,4-diamine (19)** According to General Procedure B, 2-chloro-6-methylpyridin-4-amine (0.18 g, 1.28 mmol) and 3,5-dichloroaniline (0.41 g, 2.56 mmol) yielded compound **19** as a purple oil (0.07 g, 20%). ^{1}H NMR (400 MHz, Methanol-*d*$_4$) δ 7.26 (t, *J* = 1.8 Hz, 1H), 7.22 (d, *J* = 1.8 Hz, 2H), 6.21 (d, *J* = 2.1, Hz, 1H), 6.16 (d, *J* = 2.1 Hz, 1H), 2.33 (s, 3H). ^{13}C NMR (101 MHz, CD$_3$OD) δ 156.9, 156.1, 155.1, 144.9, 134.6, 118.8, 115.3, 103.1, 92.0, 22.4. LC/MS (ESI) calcd for C$_{12}$H$_{11}$Cl$_2$N$_3$ (M + H)$^+$ 268.0, found 268.0.

***N*^{4}-(3,5-Dichlorophenyl)-6-methylpyridine-2,4-diamine (20)** According to General Procedure B, 4-chloro-6-methylpyridin-2-amine (0.25 g, 1.75 mmol) and 3,5-dichloroaniline (0.426 g, 2.62 mmol) yielded compound **20** as an off-white foam (0.09 g, 19%). ^{1}H NMR (400 MHz, Methanol-*d*$_4$) δ 7.26 (t, *J* = 1.8 Hz, 1H), 7.22 (d, *J* = 1.8 Hz, 2H), 6.21 (d, *J* = 2.7 Hz, 1H), 6.16 (d, *J* = 2.7 Hz, 1H), 2.33 (s, 3H). ^{13}C NMR (101 MHz, CD$_3$CN) δ 154.9, 148.3, 141.1, 136.2, 135.3, 124.3, 120.6, 102.1, 88.2, 18.6. LC/MS (ESI) calcd for C$_{11}$H$_{12}$Cl$_2$N$_3$ (M + H)$^+$ 268.1, found 268.1.

N^4-(3,5-Dichlorophenyl)pyridine-2,4-diamine (21) 4-Chloropyridin-2-amine (1.00 g, 7.76 mmol) and 3,5-dichloroaniline (1.23 g, 7.76 mmol) were dissolved in 22 mL of a 50:50 mixture of MeOH/H_2O in a sealed tube. To this solution was added 1 mL of conc. HCl and the tube was sealed and heated to 100 °C for 18 h. After cooling to rt, the volatiles were concentrated *in vacuo*. The residual oil was partitioned between 30 mL of EtOAc and 30 mL of 10 % NaOH. The layers were separated and the aqueous layer was extracted with 3 × 30 mL of EtOAc. The combined organic layers were dried (Na_2SO_4) and concentrated. The resulting oil was purified by flash chromatography (0–10% MeOH/DCM) to give amine **21** as an off-white foam (0.41 g, 21%). ^{1}H NMR (400 MHz, Methanol-d_4) δ 7.66 (d, J = 5.9 Hz, 1H), 7.10 (s, 2H), 7.00 (s, 1H), 6.30–6.24 (m, 2H). ^{13}C NMR (101 MHz, Methanol-d_4) δ 160.3, 151.2, 146.7, 143.7, 135.2, 121.1, 117.3, 102.6, 92.4. LC/MS (ESI) calcd for $C_{11}H_{10}Cl_2N_3$ (M+H)$^+$ 254.0, found 254.0.

N^4-(3,5-Dichlorophenyl)pyridine-3,4-diamine (22) According to General Procedure B, 4-chloropyridin-3-amine (0.835 g, 6.50 mmol) and 3,5-dichloroaniline (1.58 g, 9.73 mmol) yielded compound **22** as a yellow solid (0.53 g, 32%). ^{1}H NMR (400 MHz, CD$_3$OD) δ 7.95 (s, 1H), 7.73 (d, J = 5.5 Hz, 1H), 7.06 (d, J = 5.5 Hz, 1H), 6.97 (d, J = 1.8 Hz, 2H), 6.93 (t, J = 1.8 Hz, 1H). ^{13}C NMR (101 MHz, CD$_3$OD) δ 144.6, 138.6, 136.3, 135.5, 135.2, 121.6, 120.3, 116.0, 111.9.

N-(3,5-Dichlorophenyl)-6-methylpyrimidin-4-amine (23) According to General Procedure A, 4-chloro-6-methylpyrimidine (0.69 g, 5.37 mmol) and 3,5-dichloroaniline (0.87 g, 5.37 mmol) yielded compound **23** (0.86 g, 63 %) as a white foam. ^{1}H NMR (400 MHz, Methanol-d_4) δ 8.55 (s, 1H), 7.74 (s, 2H), 7.03 (s, 1H), 6.62 (s, 1H), 2.37 (s, 3H). ^{13}C NMR (101 MHz, Methanol-d_4) δ 164.7, 160.6, 157.0, 142.0, 134.6, 121.5, 117.5, 105.9, 21.9. LC/MS (ESI) calcd for $C_{11}H_{10}Cl_2N_3$ (M + H)$^+$ 254.0, found 254.0.

N^4-(3,5-Dichlorophenyl)-N^2,6-dimethylpyrimidine-2,4-diamine (24) According to

General Procedure A, 4-chloro-N,6-dimethylpyrimidin-2-amine (0.53 g, 3.37 mmol) and 3,5-

dichloroaniline (0.55 g, 3.37 mmol) yielded compound **24** (0.56 g, 67%) as an off-white solid;

mp 200–201 °C. ^{1}H NMR (400 MHz, Methanol-d_4) δ 7.81 (s, 2H), 6.95 (s, 1H), 5.87 (s, 1H),

2.94 (s, 3H), 2.18 (s, 3H). ^{13}C NMR (101 MHz, Methanol-d_4) δ 164.8, 162.1, 161.4, 142.7,

134.4, 120.6, 117.1, 95.1, 27.2, 21.7. LC/MS (ESI) calcd for $C_{12}H_{13}Cl_2N_4$ (M+H)$^+$ 283.1, found

283.1.

N^4-(3,5-Dichlorophenyl)-N^2,N^2,6-trimethylpyrimidine-2,4-diamine (25) According to

General Procedure A, 4-chloro-N,N,6-trimethylpyrimidin-2-amine (0.86 g, 4.98 mmol) and 3,5-

dichloroaniline (0.81 g, 4.98 mmol) yielded compound **25** (0.63 g, 48%) as an off-white foam.

^{1}H NMR (400 MHz, Methanol-d_4) δ 7.72 (s, 2H), 6.85 (s, 1H), 5.77 (s, 1H), 3.10 (s, 6H), 2.17 (s,

3H). ^{13}C NMR (101 MHz, Methanol-d_4) δ 165.4, 161.8, 160.6, 142.9, 134.3, 120.1, 116.7, 94.6,

36.4, 22.4. LC/MS (ESI) calcd for $C_{13}H_{15}Cl_2N_4$ (M+H)$^+$ 297.1, found 297.1.

N^4-(3,5-Dichlorophenyl)pyrimidine-2,4,6-triamine (26) According to General Procedure

C, 6-chloropyrimidine-2,4-diamine (1.00 g, 6.91 mmol) and 3,5-dichloroaniline (1.46 g, 8.99

mmol) yielded compound **26** as an off-white solid (0.95 g, 51%); mp 119–120 °C. ^{1}H NMR (500

MHz, DMSO-d_6) δ 8.97 (s, 1H), 7.75 (d, J = 1.8 Hz, 2H), 6.95 (t, J = 1.8 Hz, 1H), 6.04 (s, 2H),

5.92 (s, 2H), 5.21 (s, 1H). ^{13}C NMR (126 MHz, DMSO-d_6) δ 165.0, 163.1, 161.2, 144.7, 134.2,

119.3, 116.6, 78.1. LC/MS (ESI) calcd for $C_{10}H_{10}Cl_2N_5$ (M + H)$^+$ 270.0, found 270.0.

N^4-(3-Bromo-5-chlorophenyl)-2-methylpyrimidine-4,6-diamine (27) According to

General Procedure A, 6-chloro-2-methylpyrimidin-4-amine (0.50 g, 3.48 mmol) and 3-chloro-5-

bromoaniline (0.94 g, 4.52 mmol) yielded compound **27** as a white solid (0.82 g, 75%); mp 178–

179 °C. ^{1}H NMR (400 MHz, Methanol-d_4) δ 7.69 (t, J = 1.8 Hz, 1H), 7.61 (t, J = 1.8 Hz, 1H),

7.10 (t, J = 1.8 Hz, 1H), 5.72 (s, 1H), 2.34 (s, 3H). ^{13}C NMR (101 MHz, Methanol-d_4) δ 166.1, 163.6, 160.5, 143.0, 134.7, 123.6, 122.1, 120.3, 117.8, 82.8, 23.7. LC/MS (ESI) calcd for $C_{11}H_{10}BrClN_4$ (M + H)[+] 313.0, found 313.0.

N^4-(3,5-Dichlorophenyl)-N^4,6-dimethylpyrimidine-2,4-diamine (28) According to General Procedure A, pyrimidineamine (0.56 g, 2.83 mmol) and 3,5-dichloro-N-methylaniline (0.41 g, 2.83 mmol) yielded compound **28** (0.47 g, 59%) as an off-white solid; mp 156-157 °C. ^{1}H NMR (400 MHz, Methanol-d_4) δ 7.39 (t, J = 1.9 Hz, 1H), 7.30 (d, J = 1.9 Hz, 2H), 5.73 (s, 1H), 3.38 (s, 3H), 2.13 (s, 3H). ^{13}C NMR (101 MHz Methanol-d_4) δ 164.3, 163.5, 161.9, 147.0, 135.4, 126.3, 125.7, 93.7, 37.0, 21.6. LC/MS (ESI) calcd for $C_{12}H_{13}Cl_2N_4$ (M+H)[+] 283.1, found 283.1.

4-((3,5-Dichlorophenyl)thio)-6-methylpyrimidin-2-amine (29) To a stirred solution of 4-chloro-6-methylpyrimidin-2-amine (0.45 g, 3.11 mmol) and 3,5-dichlorothiophenol (0.56 g, 3.11 mmol) in 6.2 mL of DMF was added Et$_3$N (0.87 mL, 6.22 mmol). The solution was stirred at rt for 24 h The mixture was partitioned between 20 mL of EtOAc and 20 mL of H$_2$O. The layers were separated and the aqueous layer was extracted with 3 × 20 mL of EtOAc. The combined organic layers were dried (Na$_2$SO$_4$) and concentrated. The resulting dark oil was purified by flash chromatography (0–50% EtOAc/Hexanes) to afford thioether **29** as a white foam (0.58 g, 65%). ^{1}H NMR (400 MHz, CDCl$_3$) δ 7.44 (d, J = 1.9 Hz, 2H), 7.39 (t, J = 1.9 Hz, 1H), 6.04 (s, 1H), 5.59 (br s, 2H), 2.18 (s, 3H). ^{13}C NMR (101 MHz, CDCl$_3$) δ 170.2, 167.63 162.2, 135.5, 133.2, 131.9, 129.7, 106.9, 23.8. LC/MS (ESI) calcd for $C_{11}H_{10}Cl_2N_3S$ (M+H)[+] 286.0, found 286.0.

N^4-(3,5-Dichlorobenzyl)-6-methylpyrimidine-2,4-diamine (30) 4-Chloro-6-methylpyrimidin-2-amine (0.68 g, 4.73 mmol) and (3,5-dichlorophenyl)methanamine (1.00 g,

5.67 mmol) were charged into a microwave vial followed by DIPEA (1.65 mL, 9.46 mmol) and 8 mL of CH₃CN. The vial was capped and heated to 140 °C for 2 h in the microwave. After cooling to rt, the volatiles were concentrated *in vacuo*. The residual oil was partitioned between 20 mL of EtOAc and 20 mL of 10% NaOH. The layers were separated and the aqueous layer was extracted with 3 × 20 mL of EtOAc. The combined organic layers were dried (Na₂SO₄) and concentrated. The resulting dark oil was purified by flash chromatography (0–10% MeOH/DCM) to give amine **30** as a white solid (0.66 g, 49%); mp 129–130 °C. ¹H NMR (400 MHz, Methanol-*d₄*) *δ* 7.17 (app s, 3H), 5.69 (s, 1H), 4.44 (s, 2H), 2.06 (s, 3H). ¹³C NMR (101 MHz, CD₃OD) *δ* 164.3, 163.8, 162.7, 143.8, 134.6, 126.4, 125.4, 94.2, 47.3, 42.7, 21.0. LC/MS (ESI) calcd for C₁₂H₁₃Cl₂N₄ (M + H)⁺ 283.0, found 283.0.

***N*⁴-(3,5-Dichlorophenethyl)-6-methylpyrimidine-2,4-diamine (31)** 4-Chloro-6-methylpyrimidin-2-amine (0.22 g, 1.53 mmol) and 2-(3,5-dichlorophenyl)ethan-1-amine (0.35 g, 1.83 mmol) were charged into a microwave vial followed by DIPEA (0.5 mL, 3.06 mmol) and 4 mL of CH₃CN. The vial was capped and heated to 140 °C for 2 h in the microwave. After cooling to rt, the volatiles were concentrated *in vacuo*. The residual oil was partitioned between 20 mL of EtOAc and 20 mL of 10% NaOH. The layers were separated and the aqueous layer was extracted with 3 × 20 mL of EtOAc. The combined organic layers were dried (Na₂SO₄) and concentrated. The resulting dark oil was purified by flash chromatography (0–10% MeOH/DCM) to give amine **31** as a clear oil (0.29 g, 64%). ¹H NMR (400 MHz, CD₃CN) *δ* 7.30 (d, *J* = 1.9 Hz, 1H), 7.22 (t, *J* = 1.9 Hz, 2H), 6.09 (s, 1H), 5.71 (s, 1H), 4.08 (br s, 2H), 3.52 (q, *J* = 6.7 Hz, 2H), 2.84 (t, *J* = 6.7 Hz, 2H), 2.10 (s, 3H). ¹³C NMR (101 MHz, CD₃CN) *δ* 163.9, 143.8, 134.3, 134.3, 127.6, 126.0, 125.9, 93.5, 41.2, 34.6, 34.4. LC/MS (ESI) calcd for C₁₃H₁₅Cl₂N₄ (M + H)⁺ 297.1, found 297.1.

N^4-(3-Bromo-5-chlorophenyl)-6-methylpyrimidine-2,4-diamine (32) According to General Procedure C, 4-chloro-6-methylpyrimidin-2-amine (1.32 g, 8.07 mmol) and 3-bromo-5-chloroaniline (2.00 g, 9.68 mmol) yielded compound **32** as a white solid (2.20 g, 87%); mp 155–156 °C. ^{1}H NMR (400 MHz, DMSO-d_6) δ 9.28 (s, 1H), 7.89 (t, J = 1.9 Hz, 1H), 7.84 (t, J = 1.9 Hz, 1H), 7.13 (t, J = 1.9 Hz, 1H), 6.32 (s, 2H), 5.83 (s, 1H), 2.08 (s, 3H). ^{13}C NMR (101 MHz, DMSO-d_6) δ 166.3, 163.2, 161.2, 144.0, 134.5 123.0, 122.4, 119.9, 117.5, 95.9, 23.9. LC/MS (ESI) calcd for $C_{11}H_{11}BrClN_4$ (M + H)$^+$ 313.0, found 313.0.

3-((2-Amino-6-methylpyrimidin-4-yl)amino)-5-chlorobenzonitrile (33) According to General Procedure C, 4-chloro-6-methylpyrimidin-2-amine (0.47 g, 2.73 mmol) and 3-chloro-5-cyanoaniline (0.50 g, 3.27 mmol) yielded compound **33** as an off-white solid (0.52 g, 73%); mp270–271 °C. ^{1}H NMR (400 MHz, DMSO-d_6) δ 9.46 (s, 1H), 8.21 (t, J = 1.8 Hz, 1H), 8.01 (t, J = 1.8 Hz, 1H), 7.45 (t, J = 1.8 Hz, 1H), 6.41 (s, 2H), 5.85 (s, 1H), 2.09 (s, 3H). ^{13}C NMR (101 MHz, DMSO-d_6) δ 166.6, 163.2, 161.1, 143.6, 134.4, 123.7, 122.7, 120.4, 118.3, 113.5, 95.9, 24.0. LC/MS (ESI) calcd for $C_{11}H_{11}ClN_5$ (M + H)$^+$ 260.1, found 260.1.

N^4-(3-Chloro-5-(trifluoromethyl)phenyl)-6-methylpyrimidine-2,4-diamine (34) According to General Procedure C, 4-chloro-6-methylpyrimidin-2-amine (0.38 g, 2.64 mmol) and 3-chloro-5-trifluromethylaniline (0.62 g, 3.17 mmol) yielded compound **34** as a white solid (0.62 g, 81%); mp 159–160 °C. ^{1}H NMR (400 MHz, DMSO-d_6) δ 9.47 (s, 1H), 8.30 (t, J = 1.9 Hz, 1H), 7.84 (t, J = 1.9 Hz, 1H), 7.25 (t, J = 1.9 Hz, 1H), 6.34 (br s, 2H), 5.85 (s, 1H), 2.09 (s, 3H). ^{13}C NMR (101 MHz, DMSO- d_6) δ 166.5, 163.2, 161.2, 143.6, 134.6, 131.3 (q, J_{CF} = 32.0 Hz), 125.2, 121.7, 117.0, 113.9, 95.9, 23.9. LC/MS (ESI) calcd for $C_{12}H_{11}ClF_3N_4$ (M + H)$^+$ 303.1, found 303.1.

N^4-(5-Chloro-[1,1'-biphenyl]-3-yl)-6-methylpyrimidine-2,4-diamine (35) According to

General Procedure D, bromo-pyrimidineamine **32** (0.50 g, 1.59 mmol) and phenylboronic acid

(0.21 g, 1.75 mmol) yielded compound **35** as an off-white foam (0.33 g, 67%). ^{1}H NMR (400

MHz, CDCl$_3$) δ 7.53–7.50 (m, 2H), 7.45–7.40 (m, 3H), 7.39–7.34 (m, 2H), 7.28 (m, 1H), 6.86 (s,

1H), 5.99 (s, 1H), 4.98 (s, 2H), 2.22 (s, 3H). (101 MHz, CDCl$_3$) ^{13}C NMR (100 MHz, CDCl$_3$) δ

167.6, 162.7, 161.6, 143.7, 140.4, 139.4, 135.0, 128.9, 128.18, 127.0, 122.6, 120.1, 118.3, 95.0,

24.0. LC/MS (ESI) calcd for C$_{17}$H$_{16}$ClN$_4$ (M + H)$^+$ 311.1, found 311.1.

N^4-(3-Chloro-5-(pentafluoro-λ^6-sulfaneyl)phenyl)-6-methylpyrimidine-2,4-diamine (36)

According to General Procedure C, 4-chloro-6-methylpyrimidin-2-amine (0.14 g, 0.97 mmol)

and 3-chloro-5-(pentafluorosulfanyl)aniline (0.30 g, 1.18 mmol) yielded compound **36** as a white

solid (0.22 g, 63%); mp194–195 °C. ^{1}H NMR (400 MHz, DMSO-d_6) δ 9.55 (s, 1H), 8.43 (s, 1H),

7.95 (s, 1H), 7.39 (s, 1H), 6.40 (s, 2H), 5.86 (s, 1H), 2.10 (s, 3H). ^{13}C NMR (101 MHz, DMSO-

d_6) δ 166.6, 163.1, 161.2, 153.7 (sext, J_{CF} = 17.1 Hz), 143.3, 134.1, 121.6, 117.4 114.5, 96.0,

23.8. LC/MS (ESI) calcd for C$_{11}$H$_{11}$ClF$_5$N$_4$S (M + H)$^+$ 361.1, found 361.1.

N^4-(3-Bromo-5-(pentafluoro-λ^6-sulfaneyl)phenyl)-6-methylpyrimidine-2,4-diamine (37)

According to General Procedure C, 4-chloro-6-methylpyrimidin-2-amine (0.09 g, 0.58 mmol)

and 3-bromo-5-(pentafluorosulfanyl)aniline (0.21 g, 0.70 mmol) yielded compound **37** as a white

solid (0.21 g, 77%); mp 175–176 °C. ^{1}H NMR (400 MHz, DMSO-d_6) δ 9.54 (s, 1H), 8.48 (t, J =

1.8 Hz, 1H), 8.05 (t, J = 1.8 Hz, 1H), 7.54 (t, J = 1.8 Hz, 1H), 6.36 (s, 2H), 5.86 (s, 1H), 2.11 (s,

3H). ^{13}C NMR (101 MHz, DMSO-d_6) δ 166.6, 163.1, 161.2, 143.4, 124.5, 122.1, 120.1, 120.0,

114.9, 96.0, 23.9. LC/MS (ESI) calcd for C$_{11}$H$_{11}$BrF$_5$N$_4$S (M + H)$^+$ 405.0, found 405.0.

N^4-(3-Bromo-5-ethylphenyl)-6-methylpyrimidine-2,4-diamine (38) According to General

Procedure A, 4-chloro-6-methylpyrimidin-2-amine (0.28 g, 1.92 mmol) and 3-bromo-5-

ethylaniline (0.50 g, 2.50 mmol) yielded compound **38** as an off-white foam (0.48 g, 81%). [1]H

NMR (400 MHz, Methanol-d_4) δ 7.75 (t, J = 1.8 Hz, 1H), 7.30 (t, J = 1.8 Hz,1H), 6.96 (t, J = 1.8

Hz, 1H), 5.90 (s, 1H), 2.57 (q, J = 7.6 Hz, 2H), 1.19 (t, J = 7.6 Hz, 3H). ^{13}C NMR (101 MHz,

Methanol-d_4) δ 164.7, 162.5, 161.9, 146.7, 141.3, 124.4, 121.7, 120.0, 118.0, 95.6, 28.2, 21.8,

14.5. LC/MS (ESI) calcd for $C_{13}H_{16}BrN_4$ (M + H)[+] 307.1, found 307.1.

N[**4**]**-(3-Bromo-5-ethoxyphenyl)-6-methylpyrimidine-2,4-diamine (39)** According to

General Procedure A, 4-chloro-6-methylpyrimidin-2-amine (0.15 g, 1.07 mmol) and 3-bromo-5-

ethoxyaniline (0.35 g, 1.29 mmol) yielded compound **39** as a orange oil (0.25 g, 71%). ^{1}H NMR

(400 MHz, Methanol-d_4) δ 7.35 (t, J = 1.9 Hz, 1H), 7.27 (t, J = 1.9 Hz, 1H), 6.66 (t, J = 1.9 Hz,

1H), 5.90 (s, 1H), 3.98 (q, J = 7.0 Hz, 2H), 2.15 (s, 3H), 1.35 (t, J = 7.0 Hz, 3H). ^{13}C NMR (101

MHz, Methanol-d_4) δ 164.9, 162.6, 161.9, 160.0, 142.2, 122.0, 114.7, 111.0, 104.9, 95.1, 63.4,

21.8, 13.6. LC/MS (ESI) calcd for $C_{13}H_{16}BrN_4O$ (M + H)[+] 323.0, found 323.0.

N[**4**]**-(3-Bromo-5-(2,2,2-trifluoroethoxy)phenyl)-6-methylpyrimidine-2,4-diamine (40)**

According to General Procedure A, 4-chloro-6-methylpyrimidin-2-amine (0.12 g, 0.86 mmol)

and 3-bromo-5-(2,2,2-trifluoroethoxy)aniline (0.35 g, 1.29 mmol) yielded compound **40** as a

white solid (0.21 g, 65%); mp 94–95 °C. ^{1}H NMR (400 MHz, Methanol-d_4) δ 7.53–7.44 (m, 2H),

6.87 (s, 1H), 5.96 (s, 1H), 4.54 (q, J_{HF} = 8.6 Hz, 2H), 2.22 (s, 3H). ^{13}C NMR (101 MHz,

Methanol-d_4) δ 162.1, 159.9, 158.3, 141.6, 125.0, 122.2, 116.7, 112.1, 105.8, 96.4, 65.2 (q, J_{CF} =

35.4 Hz), 19.7. LC/MS (ESI) calcd for $C_{13}H_{13}BrF_3N_4O$ (M + H)[+] 377.0, found 377.0.

N[**4**]**-(3-(Allyloxy)-5-bromophenyl)-6-methylpyrimidine-2,4-diamine (41)** According to

General Procedure A, 4-chloro-6-methylpyrimidin-2-amine (0.15 g, 1.01 mmol) and 3-

(allyloxy)-5-bromoaniline (0.30 g, 1.32 mmol) yielded compound **41** as an off-white foam (0.25

g, 73%). ^{1}H NMR (400 MHz, Acetone-d_6) δ 8.38 (s, 1H), 7.57–7.43 (m, 2H), 6.70 (s, 1H), 6.01

(m, 1H), 5.93-5.86 (m 3H), 5.40 (dd, $J = 17.4$, 1.8 Hz, 1H), 5.24 (dd, $J = 10.6$, 1.8 Hz, 1H), 4.57

(d, $J = 5.5$ Hz, 2H), 2.10 (s, 3H). ^{13}C NMR (101 MHz, Acetone-d_6) δ 166.2, 163.2, 161.6, 159.8,

143.2, 133.4, 121.9, 116.8, 114.5, 110.9, 104.8, 95.5, 68.6, 22.9. LC/MS (ESI) calcd for

$C_{14}H_{16}BrN_4O$ (M + H)$^+$ 335.0, found 335.0.

N^4-(3-Bromo-5-butoxyphenyl)-6-methylpyrimidine-2,4-diamine (42) According to

General Procedure A, 4-chloro-6-methylpyrimidin-2-amine (0.14 g, 0.94 mmol) and 3-bromo-5-

butoxyaniline (0.30 g, 1.23 mmol) yielded compound **42** as a tan oil (0.2 g, 61%). ^{1}H NMR (400

MHz, Acetone-d_6) δ 8.35 (s, 1H), 7.53 (s, 1H), 7.37 (s, 1H), 6.68 (s, 1H), 5.94 (s, 1H), 5.85 (s,

2H), 3.99 (t, $J = 5.6$ Hz, 2H), 2.11 (s, 3H), 1.81–1.63 (m, 2H), 1.56–1.41 (m, 2H), 0.95 (t, $J = 5.8$

Hz, 3H). ^{13}C NMR (101 MHz, Acetone-d_6) δ 166.2, 163.2, 161.7, 160.3, 143.2, 122.0, 114.3,

110.7, 104.5, 95.5, 67.7, 31.1, 22.9, 18.9, 13.2. LC/MS (ESI) calcd for $C_{15}H_{20}BrN_4O$ (M + H)$^+$

351.1, found 351.1.

N^4-(3-Bromo-5-isobutoxyphenyl)-6-methylpyrimidine-2,4-diamine (43) According to

General Procedure A, 4-chloro-6-methylpyrimidin-2-amine (0.14 g, 0.99 mmol) and 3-bromo-5-

isobutoxyaniline (0.30 g, 1.22 mmol) yielded compound **43** as a tan oil (0.22 g, 65%). ^{1}H NMR

(400 MHz, Acetone-d_6) δ 8.38 (s, 1H), 7.56 (s, 1H), 7.33 (s, 1H), 6.69 (s, 1H), 6.09–5.84 (m,

3H), 3.74 (d, $J = 6.8$ Hz, 2H), 2.11 (s, 3H), 2.04 (m, 1H), 0.99 (d, $J = 6.8$ Hz, 6H). ^{13}C NMR

(101 MHz, Acetone-d_6) δ 166.2, 163.3, 161.7, 160.4, 143.1, 122.0, 114.4, 110.8, 104.6, 95.5,

74.3, 28.0, 22.9, 18.5. LC/MS (ESI) calcd for $C_{15}H_{20}BrN_4O$ (M + H)$^+$ 351.1, found 351.1.

N^4-(3,5-Dibromophenyl)-6-methylpyrimidine-2,4-diamine (44) According to General

Procedure C, 4-chloro-6-methylpyrimidin-2-amine (1.08 g, 6.64 mmol) and 3,5-dibromoaniline

(2.00 g, 7.97 mmol) yielded compound **44** as an off-white solid (1.92 g, 81%); mp 179–180 °C.

^{1}H NMR (400 MHz, DMSO-d_6) δ 9.25 (s, 1H), 7.95 (d, $J = 1.8$ Hz, 2H), 7.21 (t, $J = 1.8$ Hz, 1H),

6.39 (s, 2H), 5.85 (s, 1H), 2.08 (s, 3H). ^{13}C NMR (101 MHz, DMSO-d_6) δ 166.3, 163.2, 161.3, 144.1, 125.6, 122.6, 120.3, 96.0, 23.8. LC/MS (ESI) calcd for $C_{11}H_{11}Br_2N_4$ (M + H)$^+$ 357.0, found 357.0.

N^4-(3,5-Bis(methylsulfonyl)phenyl)-6-methylpyrimidine-2,4-diamine (45) According to General Procedure C, 4-chloro-6-methylpyrimidin-2-amine (0.24 g, 1.67 mmol) and 3,5-bis(methylsulfonyl)aniline (0.50 g, 2.00 mmol) yielded compound **45** as a white solid (0.35 g, 59%); mp >290 °C. ^{1}H NMR (400 MHz, DMSO-d_6) δ 9.80 (s, 1H), 8.50 (t, J = 1.5 Hz, 2H), 7.86 (d, J = 1.5 Hz, 1H), 6.34 (s, 2H), 5.91 (s, 1H), 3.33 (s, 6H), 2.12 (s, 3H). ^{13}C NMR (101 MHz, DMSO-d_6) δ 166.8, 163.1, 161.1, 143.2, 142.8, 121.3, 117.0, 96.0, 43.7, 24.0. LC/MS (ESI) calcd for $C_{13}H_{17}N_4O_4S_2$ (M + H)$^+$ 357.1, found 357.1.

N^4-(3,5-Bis(trifluoromethyl)phenyl)-6-methylpyrimidine-2,4-diamine (46) According to General Procedure A, pyrimidineamine (1.22 g, 8.52 mmol) and 3,5-bis-trifluoromethylaniline (1.32 g, 8.52 mmol) yielded compound **46** (1.57 g, 55%) as white solid; mp 119–120 °C. 1H NMR (400 MHz, Methanol-d_4) δ 8.31 (s, 2H), 7.56 (s, 1H), 6.05 (s, 1H), 2.27 (s, 3H). ^{13}C NMR (101 MHz, Methanol-d_4) δ 162.1, 160.2, 159.7, 141.2, 132.21, 131.9; 131.7 (q, J = 33.2 Hz); 131.6, 131.2, 127.4, 124.7, 121.9, 119.5, 115.3, 96.7, 20.6. LC/MS (ESI) calcd for $C_{13}H_{11}F_6N_4$ (M+H)$^+$ 337.1, found 337.1.

N^4-(3,5-Dimethoxyphenyl)-6-methylpyrimidine-2,4-diamine (47) According to General Procedure A, 4-chloro-6-methylpyrimidin-2-amine (0.72 g, 5.00 mmol) and 3,5-dimethoxyaniline (0.76 g, 5.00 mmol) yielded amine **47** as a white solid (1.08 g, 83%); mp 184–185 °C. ^{1}H NMR (400 MHz, CD$_3$OD) δ 6.81 (d, J = 2.3 Hz, 2H), 6.17 (t, J = 2.3 Hz, 1H), 5.94 (s, 1H), 3.75 (s, 6H), 2.15 (s, 3H). ^{13}C NMR (101 MHz, CD$_3$OD) δ 164.6, 162.6, 162.2, 161.0,

141.4, 98.6, 95.4, 94.5, 54.3, 21.8. LC/MS (ESI) calcd for $C_{11}H_{10}Cl_2N_3$ (M + H)$^+$ 254.0, found 254.0.

5-((2-Amino-6-methylpyrimidin-4-yl)amino)isophthalic acid (48) According to General Procedure A, 4-chloro-6-methylpyrimidin-2-amine (1.00 g, 6.69 mmol) and 5-aminoisophthalic acid (1.21 g, 6.69 mmol) yielded compound **48** as a white solid (1.25 g, 65%); mp >300 °C. ^{1}H NMR (400 MHz, DMSO-d_6) δ 13.13 (br s, 2H), 11.18 (br s, 1H), 8.38 (s, 2H), 8.21–8.18 (m, 3H), 6.27 (s, 1H), 2.26 (s, 3H). ^{13}C NMR (101 MHz, DMSO-d_6) δ 167.0, 162.3, 156.2, 153.5, 138.9, 132.4, 126.8, 126.2, 97.9, 18.7. LC/MS (ESI) calcd for $C_{13}H_{13}N_4O_4$ (M + H)$^+$ 289.1, found 289.1.

Dimethyl 5-((2-amino-6-methylpyrimidin-4-yl)amino)isophthalate (49) To a stirred solution of 5-((2-amino-6-methylpyrimidin-4-yl)amino)isophthalic acid **48** (0.05 g, 0.17 mmol) in 25 mL of MeOH was added 0.8 mL of conc. H_2SO_4. 4Å molecular sieves were added and the solution was heated to reflux for 18 h. After cooling to rt, the volatiles were concentrated *in vacuo*. The residual oil was partitioned between 20 mL of EtOAc and 20 mL of 10% NaOH. The layers were separated and the aqueous layer was extracted with 3 × 20 mL of EtOAc. The combined organic layers were dried (Na_2SO_4) and concentrated. The resulting dark oil was purified by flash chromatography (0–10% MeOH/DCM) to give amine **49** as a white foam (0.05 g, 93%). ^{1}H NMR (400 MHz, DMSO-d_6) δ 9.43 (s, 1H), 8.51 (d, J = 1.6 Hz, 2H), 8.00 (t, J = 1.6 Hz, 1H), 6.13 (s, 2H), 5.86 (s, 1H), 3.86 (s, 6H), 2.09 (s, 3H). ^{13}C NMR (101 MHz, DMSO-d_6) δ 166.7, 166.3, 166.0, 163.2, 142.2, 131.0, 123.9, 122.3, 95.8, 52.9, 23.9. LC/MS (ESI) calcd for $C_{15}H_{17}N_4O_4$ (M + H)$^+$ 317.1, found 317.1.

N^4**-([1,1':3',1''-Terphenyl]-5'-yl)-6-methylpyrimidine-2,4-diamine (50)** According to General Procedure D, dibromo-pyrimidineamine **44** (0.5 g, 1.40 mmol) and phenylboronic acid

(0.41 g, 3.35 mmol) yielded compound **50** as a yellow foam (0.36 g, 72%). ^{1}H NMR (500 MHz, CDCl$_3$) δ 7.65–7.62 (m, 4H), 7.61–7.58 (m, 2H), 7.52 (d, J = 1.6 Hz, 2H), 7.50–7.45 (m, 4H), 7.43–7.38 (m, 2H), 6.10 (s, 1H), 5.29 (s, 2H), 2.24 (s, 3H). ^{13}C NMR (126 MHz, CDCl$_3$) δ 167.4, 162.9, 162.4, 142.9, 140.6, 139.6, 128.9, 127.7, 127.2, 122.29, 120.2, 94.4, 24.0. LC/MS (ESI) calcd for C$_{23}$H$_{21}$N$_4$ (M + H)$^+$ 353.2, found 353.2.

5-((2-Amino-6-methylpyrimidin-4-yl)amino)-N^1,N^3-bis(3,5-dichlorophenyl)isophthalamide (51) To a solution of diacid **48** (0.32 g, 1.09 mmol) and 3,5-dichloroaniline (0.45 g, 2.74 mmol) in a solution of 3 mL pyridine, 7 mL DCM and 7 mL of DMF, was added EDI (0.63 g, 3.27 mmol). The solution was stirred at rt for 18 h before being diluted with 50 mL of water. The solution was then extracted with 3 × 50 mL of EtOAc. The combined organic layers were then washed with water followed by brine, dried (Na$_2$SO$_4$) and concentrated in vacuo to afford a brown oil. The oil was purified by flash chromatography (0–20% MeOH/DCM gradient) to afford diamide **51** as a white solid (0.43 g, 69%); mp 235–236 °C. ^{1}H NMR (500 MHz, DMSO-d_6) δ 10.71 (s, 2H), 9.48 (s, 1H), 8.41 (d, J = 1.4 Hz, 2H), 8.04 (t, J = 1.4 Hz, 1H), 7.93 (d, J = 1.9 Hz, 4H), 7.37 (t, J = 1.9 Hz, 2H), 6.23 (s, 2H), 5.96 (s, 1H), 2.14 (s, 3H). ^{13}C NMR (101 MHz, DMSO-d_6) δ 166.3, 166.2, 163.2, 161.5, 141.9, 141.9, 135.7, 134.4, 123.4, 121.9, 119.7, 118.7, 95.6, 24.0. LC/MS (ESI) calcd for C$_{25}$H$_{19}$Cl$_4$N$_6$O$_2$ (M + H)$^+$ 575.0, found 575.0.

N^4-(3,5-Dimethylphenyl)-6-methylpyrimidine-2,4-diamine (52) According to General Procedure A, pyrimidineamine (0.76 g, 6.10 mmol) and 3,5-dimethylaniline (0.88 g, 6.10 mmol) yielded compound **52** (0.85 g, 61%) as white solid; mp 163–164 °C. ^{1}H NMR (400 MHz, Methanol-d_4) δ 7.10 (s, 2H), 6.67 (s, 1H), 5.89 (s, 1H), 2.25 (s, 6H), 2.12 (s, 3H). ^{13}C NMR (101

MHz Methanol-d_4) δ 164.7, 162.7, 162.4, 139.3, 138.1, 124.5, 118.7, 94.8, 21.8, 20.1. LC/MS

(ESI) calcd for $C_{13}H_{17}N_4$ (M+H)$^+$ 229.1, found 229.1.

N^4-(3,5-Di-tert-butylphenyl)-6-methylpyrimidine-2,4-diamine (53) According to General

Procedure C, 4-chloro-6-methylpyrimidin-2-amine (0.32 g, 2.24 mmol) and 3,5-di-*tert*-

butylaniline (0.55 g, 2.68 mmol) yielded compound **53** as a white solid (0.56 g, 80%); mp 194–

195 °C. ^{1}H NMR (400 MHz, DMSO-d_6) δ 9.58 (s, 1H), 7.39 (d, J = 1.8 Hz, 2H), 7.06 (t, J = 1.8

Hz, 1H), 6.71 (s, 2H), 5.97 (s, 1H), 3.13 (s, 2H), 2.13 (m, 2H), 1.25 (s, 18H). ^{13}C NMR (101

MHz, DMSO-d_6) δ 162.1, 160.0, 159.6, 151.1, 139.0, 117.3, 115.9, 95.9, 35.0, 31.7. LC/MS

(ESI) calcd for $C_{19}H_{29}N_4$ (M + H)$^+$ 313.2, found 313.2.

6-Methyl-N^4-(3-(pentafluoro-λ^6-sulfaneyl)phenyl)pyrimidine-2,4-diamine (54)

According to General Procedure C, 4-chloro-6-methylpyrimidin-2-amine (0.27 g, 1.90 mmol)

and 3-pentafluorosulfanylaniline (0.50 g, 2.28 mmol) yielded compound **54** as a white solid

(0.24 g, 87%); mp 175–176 °C. ^{1}H NMR (400 MHz, Methanol-d_4) δ 8.05 (t, J = 2.0 Hz, 1H),

7.96 (m, 1H), 7.40–7.28 (m, 2H), 5.90 (s, 1H), 2.13 (s, 3H). ^{13}C NMR (101 MHz, Methanol-d_4) δ

165.3, 162.6, 161.8, 153.7 (sext, J_{CF} = 16.6 Hz), 140.8, 128.6, 122.6, 118.6, 116.7, 95.8, 21.9.

LC/MS (ESI) calcd for $C_{11}H_{12}F_5N_4S$ (M + H)$^+$ 327.1, found 327.1.

N^4-(3-Chlorophenyl)-6-methylpyrimidine-2,4-diamine (55) According to General

Procedure A, 4-chloro-6-methylpyrimidin-2-amine (0.73 g, 5.06 mmol) and 3-chloroaniline

(0.534 g, 5.06 mmol) yielded compound **55** (0.57 g, 48%) as white solid; mp 142–143 °C. ^{1}H

NMR (400 MHz, Methanol-d_4) δ 7.75 (s, 1H), 7.43 (d, J = 8.2 Hz, 1H), 7.16 (t, J = 8.2 Hz, 1H),

6.91 (d, J = 8.2 Hz, 1H), 5.88 (s, 1H), 2.13 (s, 3H). ^{13}C NMR (101 MHz Methanol-d_4) δ 165.1,

162.7, 161.9, 141.4, 133.9, 129.5 121.8, 119.6, 118.0, 95.7, 22.0. LC/MS (ESI) calcd for

$C_{11}H_{12}ClN_4$ (M+H)$^+$ 235.1, found 235.1.

***N^4*-(3,5-Difluorophenyl)-6-methylpyrimidine-2,4-diamine (60)** According to General Procedure A, 4-chloro-6-methylpyrimidin-2-amine (1.09 g, 7.61 mmol) and 3,5-fluoroaniline (0.98 g, 7.61 mmol) yielded compound **60** (0.97 g, 54%) as a white solid; mp 179–180 °C. ^{1}H NMR (400 MHz, Methanol-d_4) δ 7.38–7.33 (m, 2H), 6.43 (tt, J = 9.2, 2.4 Hz, 1H), 5.88 (s, 1H), 2.15 (s, 3H). ^{13}C NMR (101 MHz, Methanol-d_4) δ 165.2, 163.1 (dd, J_{CF} = 242.8, 15.2 Hz), 162.6, 161.7, 142.90 (t, J_{CF} = 13.8 Hz), 101.96 – 101.47 (m), 96.0, 95.9 (dd, J_{CF} = 52.7, 3.4 Hz); 21.9. LC/MS (ESI) calcd for $C_{11}H_{11}F_2N_4$ (M+H)[+] 237.1, found 237.1.

***N^4*-(3-Chloro-5-fluorophenyl)-6-methylpyrimidine-2,4-diamine (61)** According to General Procedure C, 3-chloro-5-fluoroaniline (0.28 g, 1.94 mmol) and 4-chloro-6-methylpyrimidin-2-amine (0.28 g, 1.94 mmol) yielded compound **61** as a white solid (0.378 g, 77%); mp 143–144 °C. ^{1}H NMR (400 MHz, Acetone-d_6) δ 8.63 (br s, 1H), 7.80 (dt, J = 10.2, 2.1 Hz, 1H), 7.53 (q, J = 2.1 Hz, 1H), 6.74 (dt, J = 10.2, 2.1 Hz, 1H), 6.15 (br s, 2H), 5.94 (s, 1H), 2.12 (s, 3H). ^{13}C NMR (101 MHz, Acetone-d_6) δ 166.6, 162.9 (d, J_{CF} = 243.6 Hz), 161.4, 163.3, 143.7 (d, J_{CF} = 13.1 Hz), 134.2 (d, J_{CF} = 13.3 Hz), 114.5 (d, J_{CF} = 2.9 Hz), 108.0 (d, J_{CF} = 25.8 Hz), 104.5 (d, J_{CF} = 27.0 Hz) 95.7, 22.90. LC/MS (ESI) calcd for $C_{10}H_{12}ClFN_4$ (M + H)[+] 253.1, found 225.1.

***N^4*-(3,5-Dichloro-4-fluorophenyl)-6-methylpyrimidine-2,4-diamine (62)** According to General Procedure C, 4-chloro-6-methylpyrimidin-2-amine (1.00 g, 6.69 mmol) and 3,5-dichloro-4-fluoroaniline (1.24 g, 6.69 mmol) yielded compound **62** as a white solid (1.55 g, 81%); mp 204–205 °C. ^{1}H NMR (400 MHz, Acetone-d_6) δ 8.48 (br s, 1H), 7.93 (d, J_{HF} = 6.1 Hz, 2H), 5.95 (br s, 2H), 5.91 (s, 1H), 2.11 (s, 3H). [3]C NMR (101 MHz, Acetone-d_6) δ 166.7, 163.1, 161.3, 148.4 (d, J = 242.2 Hz), 138.2 (d, J = 3.8 Hz), 121.1 (d, J = 17.9 Hz), 119.1, 95.5, 23.0. LC/MS (ESI) calcd for $C_{11}H_9Cl_2FN_4$ (M + H)[+] 287.0, found 287.0.

N^4-(3,5-Dibromo-4-fluorophenyl)-6-methylpyrimidine-2,4-diamine (63) According to General Procedure C, 4-chloro-6-methylpyrimidin-2-amine (0.26 g, 1.84 mmol) and 3,5-dibromo-4-fluoroaniline (0.50 g, 2.39 mmol) yielded compound **63** as a white solid (0.59 g, 85%); mp 205–206 °C. ^{1}H NMR (400 MHz, DMSO-d_6) δ 9.20 (s, 1H), 8.02 (d, J_{HF} = 5.7 Hz, 2H), 6.33 (s, 2H), 5.80 (s, 1H), 2.07 (s, 3H). ^{13}C NMR (101 MHz, DMSO-d_6) δ 166.2, 163.1, 161.2, 149.7 (d, J = 237.2 Hz), 139.6 (d, J = 3.3 Hz), 122.4, 108.8 (d, J = 22.5 Hz), 95.6, 23.9. LC/MS (ESI) calcd for $C_{11}H_{10}Br_2FN_4$ (M + H)$^+$ 374.9, found 374.9.

6-Methyl-N^4-(3,4,5-trichlorophenyl)pyrimidine-2,4-diamine (64) According to General Procedure C, 4-chloro-6-methylpyrimidin-2-amine (0.54 g, 3.79 mmol) and 3,4,5-trichloroaniline (0.80 g, 3.79 mmol) yielded compound **64** as a white solid (0.94 g, 82%); mp 219–220 °C. ^{1}H NMR (400 MHz, DMSO-d_6) δ 9.36 (s, 1H), 8.00 (s, 2H), 6.37 (s, 2H), 5.83 (s, 1H), 2.08 (s, 3H). ^{13}C NMR (101 MHz, DMSO-d_6) δ 166.5, 163.1, 161.1, 141.6, 133.0, 120.8, 118.9, 95.9, 23.9. LC/MS (ESI) calcd for $C_{11}H_{10}Cl_3N_4$ (M + H)$^+$ 303.0, found 303.3.

N^4-(3,5-Dichloro-4-methylphenyl)-6-methylpyrimidine-2,4-diamine (65) According to General Procedure C, 4-chloro-6-methylpyrimidin-2-amine (0.31 g, 2.18 mmol) and 3,5-dichloro-4-methylaniline (0.50 g, 2.84 mmol) yielded compound **65** as a white solid (0.51 g, 83%); mp 185–186 °C. ^{1}H NMR (400 MHz, DMSO-d_6) δ 9.16 (s, 1H), 7.80 (s, 2H), 6.30 (s, 2H), 5.81 (s, 1H), 2.28 (s, 3H), 2.07 (s, 3H). ^{13}C NMR (101 MHz, DMSO-d_6) δ 166.1, 163.2, 161.3, 140.7, 134.5, 125.3, 118.1, 95.7, 23.9, 16.8. LC/MS (ESI) calcd for $C_{12}H_{13}Cl_2N_4$ (M + H)$^+$ 283.1, found 283.1.

N^4-(3,5-Dichloro-4-phenoxyphenyl)-6-methylpyrimidine-2,4-diamine (66) According to General Procedure C, 4-chloro-6-methylpyrimidin-2-amine (0.09 g, 0.67 mmol) and 3,5-dichloro-4-phenoxyaniline (0.50 g, 0.78 mmol) yielded compound **66** as an off-white solid (0.20

g, 71%); mp 100–101 °C. ^{1}H NMR (400 MHz, DMSO-d_6) δ 9.35 (s, 1H), 7.96 (s, 2H), 7.48–7.23 (m, 2H), 7.07 (m, 1H), 6.78 (m, 2H), 6.35 (s, 2H), 5.85 (s, 1H), 2.09 (s, 3H). ^{13}C NMR (101 MHz, DMSO-d_6) δ 166.1, 163.1, 161.2, 157.2, 140.1, 139.6, 130.3, 128.7, 122.9, 119.1, 114.9, 95.8, 23.9. LC/MS (ESI) calcd for $C_{17}H_{15}Cl_2N_4O$ (M + H)$^+$ 361.1, found 361.1.

4-((2-Amino-6-methylpyrimidin-4-yl)amino)-2,6-dichlorophenol (67) According to General Procedure C, 4-chloro-6-methylpyrimidin-2-amine (0.62 g, 4.32 mmol) and 4-amino-2,6-dichlorophenol (1.00 g, 5.62 mmol) yielded compound **67** as an off-white solid (1.00 g, 82%); mp 250 °C (decomposes). ^{1}H NMR (500 MHz, DMSO-d_6) δ 8.99 (s, 1H), 7.72 (s, 2H), 6.25 (s, 2H), 5.80 (s, 1H), 2.09 (s, 3H). ^{13}C NMR (126 MHz, DMSO-d_6) δ 165.6, 163.2, 161.5, 143.9, 134.5, 122.8, 119.6, 95.2, 23.9. LC/MS (ESI) calcd for $C_{11}H_{11}Cl_2N_4O$ (M + H)$^+$ 285.0, found 285.0.

N^4-(3,5-Dichloro-4-(difluoromethoxy)phenyl)-6-methylpyrimidine-2,4-diamine (68) According to General Procedure C, 4-chloro-6-methylpyrimidin-2-amine (0.13 g, 0.87 mmol) and 3,5-dichloro-4-difluoromethoxy aniline (0.24 g, 1.05 mmol) yielded compound **68** as an off-white solid (0.22 g, 62%); mp 169–170 °C. ^{1}H NMR (400 MHz, DMSO-d_6) δ 9.35 (s, 1H), 7.93 (s, 2H), 7.03 (t, J_{HF} = 72.8 Hz, 1H), 6.36 (s, 2H), 5.83 (s, 1H), 2.08 (s, 3H). ^{13}C NMR (101 MHz, DMSO-d_6) δ 166.4, 163.1, 161.1, 140.9, 136.8, 128.7, 118.8, 118.0 (t, J = 261.8 Hz), 95.82, 23.91. LC/MS (ESI) calcd for $C_{12}H_{11}Cl_2F_2N_4O$ (M + H)$^+$ 335.0, found 335.0.

N^4-(3,5-Dichloro-4-(dimethylamino)phenyl)-6-methylpyrimidine-2,4-diamine (69) According to General Procedure A, 4-chloro-6-methylpyrimidin-2-amine (0.36 g, 2.50 mmol) and 2,6-dichloro-N^1,N^1-dimethylbenzene-1,4-diamine (0.62 g, 3.00 mmol) yielded compound **69** as a clear oil (0.56 g, 72%). ^{1}H NMR (400 MHz, Methanol-d_4) δ 7.60 (s, 2H), 5.85 (s, 1H), 2.77

(s, 6H), 2.12 (s, 3H). ^{13}C NMR (101 MHz, Methanol-d_4) δ 165.1, 162.6, 161.6, 139.9, 138.3, 135.3 119.7, 95.8, 41.2, 22.0. LC/MS (ESI) calcd for $C_{13}H_{16}Cl_2N_5$ (M + H)$^+$ 312.1, found 312.1.

***N*^{4}-(3,5-Dichloro-4-morpholinophenyl)-6-methylpyrimidine-2,4-diamine (70)** According to General Procedure A, 4-chloro-6-methylpyrimidin-2-amine (0.11 g, 0.75 mmol) and 3,5-dichloro-4-morpholinoaniline (0.22 g, 0.89 mmol) yielded compound **70** as a white solid (0.21 g, 81%); mp 114–115 °C. 1H NMR (400 MHz, DMSO-d_6) δ 9.19 (s, 1H), 7.76 (s, 2H), 6.29 (s, 2H), 5.81 (s, 1H), 3.71–3.54 (m, 4H), 3.11–2.98 (m, 4H), 2.07 (s, 3H). ^{13}C NMR (101 MHz, DMSO-d_6) δ 166.0, 163.1, 161.2, 140.0, 137.3, 134.9, 119.1, 95.7, 67.5, 49.9, 23.8. LC/MS (ESI) calcd for $C_{15}H_{18}Cl_2N_5O$ (M + H)$^+$ 354.1, found 354.1.

***N*^{4}-(3,5-Dichloro-4-(piperidin-1-yl)phenyl)-6-methylpyrimidine-2,4-diamine (71)** According to General Procedure A, 4-chloro-6-methylpyrimidin-2-amine (0.37 g, 2.54 mmol) and 3,5-dichloro-4-(piperidin-1-yl)aniline (0.75 g, 3.06 mmol) yielded compound **71** as a yellow foam (0.70 g, 79%). ^{1}H NMR (400 MHz, DMSO-d_6) δ 9.14 (s, 1H), 7.73 (s, 2H), 6.24 (s, 2H), 5.80 (s, 1H), 3.05 – 2.95 (m, 4H), 2.05 (s, 3H), 1.62-1.44 (m, 6H). ^{13}C NMR (101 MHz DMSO-d_6) δ 166.1, 163.2, 161.3, 139.4, 139.0, 134.7, 119.1, 95.6, 51.1, 26.8, 24.3, 23.9. LC/MS (ESI) calcd for $C_{16}H_{20}Cl_2N_5$(M + H)$^+$ 352.1, found 352.1.

2-((2-Amino-6-methylpyrimidin-4-yl)amino)-4,6-dichlorophenol (72) According to General Procedure C, 4-chloro-6-methylpyrimidin-2-amine (1.00 g, 6.96 mmol) and 2-amino-4,6-dichlorophenol (1.48 g, 8.35 mmol) yielded compound **72** as a tan solid (1.40 g, 71%); mp 216–217 °C. ^{1}H NMR (400 MHz, DMSO-d_6) δ 7.53 (d, J = 2.6 Hz, 1H), 7.13 (d, J = 2.6 Hz, 1H), 6.02 (s, 1H), 2.08 (s, 3H). ^{13}C NMR (101 MHz, DMSO-d_6) δ 166.7, 161.9, 161.1, 144.2, 131.8, 123.5, 123.4, 122.9, 120.6, 95.6, 23.7. LC/MS (ESI) calcd for $C_{11}H_{11}Cl_2N_4O$ (M + H)$^+$ 285.0, found 285.0.

N^4-(3,5-Dichloro-2,4-difluorophenyl)-6-methylpyrimidine-2,4-diamine (73) According

to General Procedure C, 4-chloro-6-methylpyrimidin-2-amine (0.30 g, 2.10 mmol) and 3,5-

dichloro-2,4-difluoroaniline (0.50 g, 2.52 mmol) yielded compound **73** as a white solid (0.63 g,

81%); mp 203–204 °C. ^{1}H NMR (400 MHz, Methanol-d_4) δ 8.38 (t, J_{HF} = 7.9 Hz, 1H), 6.03 (s,

1H), 2.18 (s, 3H). ^{13}C NMR (101 MHz, Methanol-d_4) δ 165.8, 162.6, 161.9, 122.2, 95.6, 21.9

(halogenated carbons not visible). LC/MS (ESI) calcd for $C_{11}H_8Cl_2F_2N_4$ (M + H)$^+$ 305.0, found

305.0.

N^4-(3',5'-Dichloro-[1,1'-biphenyl]-4-yl)-6-methylpyrimidine-2,4-diamine (89) According

to General Procedure C, 4-chloro-6-methylpyrimidin-2-amine (0.38 g, 2.62 mmol) and 3',5'-

dichloro-[1,1'-biphenyl]-4-amine (0.75 g, 3.15 mmol) yielded compound **89** as a white solid

(0.69 g, 76%); mp 237–238 °C. ^{1}H NMR (400 MHz, DMSO-d_6) δ 9.16 (s, 1H), 7.81 (d, J = 8.0

Hz, 2H), 7.65 (s, 2H), 7.61 (d, J = 8.0 Hz, 2H), 7.46 (s, 1H), 6.20 (br s, 2H), 5.90 (s, 1H), 2.08 (s,

3H). ^{13}C NMR (101 MHz, DMSO-d_6) δ 165.7, 163.3, 161.5, 144.0, 142.1, 135.0, 129.9, 127.6,

126.3, 125.0, 119.7, 95.6, 23.9. LC/MS (ESI) calcd for $C_{17}H_{15}Cl_2N_4$ (M + H)$^+$ 345.1, found

345.1.

N^4-(5-Chloro-4'-fluoro-[1,1'-biphenyl]-3-yl)-6-methylpyrimidine-2,4-diamine (91)

According to General Procedure D, bromo-pyrimidineamine **32** (0.3 g, 0.95 mmol) yielded

compound **91** as an off-white solid (0.20 g, 65%); mp 105–106 °C. ^{1}H NMR (400 MHz,

Methanol-d_4) δ 7.81 (t, J = 1.9 Hz, 1H), 7.62 (t, J = 1.9 Hz, 1H), 7.60–7.55 (m, 2H), 7.17–7.11

(m, 3H), 5.92 (s, 1H), 2.16 (s, 3H). ^{13}C NMR (101 MHz, Methanol-d_4) δ 165.1, 164.0, 162.8 (d,

J_{CF} = 245.9 Hz), 161.9, 141.9 (d, J_{CF} = 16.2 Hz), 135.99, 135.95, 134.4, 128.5 (d, J_{CF} = 8.2 Hz),

120.0, 118.1, 116.2, 115.2 (d, J_{CF} = 21.9 Hz), 95.7, 21.8. LC/MS (ESI) calcd for $C_{17}H_{15}ClFN_4$

(M + H)$^+$ 329.1, found 329.1.

N^4-(4',5-Dichloro-[1,1'-biphenyl]-3-yl)-6-methylpyrimidine-2,4-diamine (92) According

to General Procedure D, bromo-pyrimidineamine **32** (0.50 g, 1.59 mmol) yielded compound **92**

as a yellow foam (0.39 g, 72%). ^{1}H NMR (400 MHz, DMSO-d_6) δ 9.26 (s, 1H), 7.93 (t, J = 1.8

Hz, 1H), 7.83 (t, J = 1.8 Hz, 1H), 7.66 (d, J = 8.5 Hz, 2H), 7.47 (d, J = 8.5 Hz, 2H), 7.20 (t, J =

1.8 Hz, 1H), 6.32 (s, 2H), 5.88 (s, 1H), 2.09 (s, 3H). ^{13}C NMR (101 MHz, DMSO-d_6) δ 166.0,

163.2, 161.6, 143.2, 141.3, 138.2, 134.3, 133.3, 129.4, 129.0, 119.2, 117.9, 116.0, 95.8, 23.9.

LC/MS (ESI) calcd for $C_{17}H_{15}Cl_2N_4$ (M + H)$^+$ 345.1, found 345.1.

N^4-(5-Chloro-4'-methoxy-[1,1'-biphenyl]-3-yl)-6-methylpyrimidine-2,4-diamine (93)

According to General Procedure D, bromo-pyrimidineamine **32** (0.46 g, 1.45 mmol) yielded

compound **93** as a yellow foam (0.30 g, 61%). ^{1}H NMR (400 MHz, DMSO-d_6) δ 9.20 (s, 1H),

7.90 (t, J = 1.8 Hz, 1H), 7.71 (t, J = 1.8 Hz, 1H), 7.58 (d, J = 8.8 Hz, 2H), 7.15 (t, J = 1.8Hz,

1H), 7.00 (d, J = 8.8 Hz, 2H), 6.25 (s, 2H), 5.87 (s, 1H), 3.77 (s, 3H), 2.08 (s, 3H). ^{13}C NMR

(101 MHz, DMSO-d_6) δ 166.0, 163.2, 161.6, 159.7, 143.1, 142.3, 134.1, 131.6, 128.3, 118.8,

117.0, 115.5, 114.8, 95.7, 55.6, 23.9. LC/MS (ESI) calcd for $C_{18}H_{18}ClN_4O$ (M + H)$^+$ 341.1,

found 341.1.

N^4-(5-Chloro-4'-methyl-[1,1'-biphenyl]-3-yl)-6-methylpyrimidine-2,4-diamine (94)

According to General Procedure D, bromo-pyrimidineamine **32** (0.50 g, 1.59 mmol) yielded

compound **94** as a yellow oil (0.40 g, 81%). ^{1}H NMR (400 MHz, DMSO-d_6) δ 9.23 (s, 1H), 7.98

(t, J = 1.8 Hz, 1H), 7.73 (t, J = 1.8 Hz, 1H), 7.52 (d, J = 8.0 Hz, 2H), 7.23 (d, J = 8.0 Hz, 2H),

7.16 (t, J = 1.8 Hz, 1H), 6.30 (s, 2H), 5.89 (s, 1H), 2.30 (s, 3H), 2.09 (s, 3H). ^{13}C NMR (101

MHz, DMSO-d_6) δ 166.0, 163.3, 161.6, 143.1, 142.6, 137.8, 136.5, 134.1, 130.0, 127.0, 119.1,

117.4, 115.8, 95.8, 23.9, 21.1. LC/MS (ESI) calcd for $C_{18}H_{18}ClN_4$ (M + H)$^+$ 325.1, found 325.1.

N^4-(5-Chloro-4'-(trifluoromethyl)-[1,1'-biphenyl]-3-yl)-6-methylpyrimidine-2,4-diamine (95) According to General Procedure D, bromo-pyrimidineamine 32 (0.5 g, 1.59 mmol) yielded compound 95 as a yellow foam (0.41 g, 67%). ^{1}H NMR (400 MHz, DMSO-d_6) δ 9.31 (s, 1H), 7.96 (m, 2H), 7.85 (d, J = 8.3 Hz, 2H), 7.76 (d, J = 8.3 Hz, 2H), 7.25 (t, J = 1.7 Hz, 1H), 6.38 (s, 2H), 5.91 (s, 1H), 2.10 (s, 3H). ^{13}C NMR (101 MHz, DMSO-d_6) δ 166.0, 163.3, 161.6, 143.4, 141.0, 134.3, 128.0, 128.8 (q, J_{CF} = 31.9 Hz), 126.2 (q, J_{CF} = 3.7 Hz), 126.0, 123.3, 119.5, 118.4, 116.3, 95.9, 23.8. LC/MS (ESI) calcd for $C_{18}H_{15}ClF_3N_4$ (M + H)$^+$ 379.1, found 379.1.

3'-((2-Amino-6-methylpyrimidin-4-yl)amino)-5'-chloro-[1,1'-biphenyl]-4-carbonitrile (96) According to General Procedure D, bromo-pyrimidineamine 32 (0.3 g, 0.95 mmol) yielded compound 96 as a tan solid (0.28 g, 88%); mp 197–198 °C. ^{1}H NMR (400 MHz, DMSO-d_6) δ 9.28 (s, 1H), 7.95 (m, 1H), 7.92 (t, J = 1.8 Hz, 1H), 7.90–7.82 (m, 4H), 7.27 (t, J = 1.8 Hz, 1H), 6.32 (s, 2H), 5.87 (s, 1H), 2.09 (s, 3H). ^{13}C NMR (101 MHz, DMSO-d_6) δ 166.1, 163.2, 161.4, 143.9, 143.3 140.7, 134.5, 133.3, 128.2, 119.5, 119.2, 118.5, 116.2, 111.0, 95.8, 23.9. LC/MS (ESI) calcd for $C_{18}H_{15}ClN_5$ (M + H)$^+$ 336.1, found 336.1.

1-(3'-((2-Amino-6-methylpyrimidin-4-yl)amino)-5'-chloro-[1,1'-biphenyl]-4-yl)ethan-1-one (97) According to General Procedure D, bromo-pyrimidineamine 32 (0.3 g, 0.95 mmol) yielded compound 97 as a white solid (0.24 g, 72%); mp 225 °C (chars). ^{1}H NMR (400 MHz, DMSO-d_6) δ 9.29 (s, 1H), 8.02 (d, J = 8.3 Hz, 2H), 7.97 (s, 1H), 7.91 (s, 1H), 7.80 (d, J = 8.3 Hz, 2H), 7.29 (s, 1H), 6.28 (s, 2H), 5.87 (s, 1H), 2.59 (s, 3H), 2.09 (s, 3H). ^{13}C NMR (101 MHz, DMSO-d_6) δ 197.9, 166.1, 163.2, 161.5, 143.6, 143.3, 141.3, 136.5, 134.3, 129.4, 127.45, 119.4, 118.3, 116.2, 95.8, 27.2, 23.9. LC/MS (ESI) calcd for $C_{19}H_{18}ClN_4O$ (M + H)$^+$ 353.1, found 353.1.

3'-((2-Amino-6-methylpyrimidin-4-yl)amino)-5'-chloro-[1,1'-biphenyl]-4-ol (98)

According to General Procedure D, bromo-pyrimidineamine **32** (0.31 g, 0.99 mmol) yielded

compound **98** as a white solid (0.22 g, 69%); mp 142–143 °C. ^{1}H NMR (400 MHz DMSO-d_6) δ

9.18 (s, 1H), 7.86 (s, 1H), 7.66 (s, 1H), 7.46 (d, J = 8.0 Hz, 2H), 7.11 (s, 1H), 6.82 (d, J = 8.0 Hz,

2H), 6.24 (s, 2H), 5.86 (s, 1H), 2.08 (s, 3H). ^{13}C NMR (101 MHz, DMSO-d_6) δ 165.9, 163.2,

161.6 158.0, 143.0, 142.7, 134.0, 130.0, 128.3, 118.6, 116.7, 116. 2, 115.3, 95.7, 23.9. LC/MS

(ESI) calcd for $C_{17}H_{16}ClN_4O$ (M + H)$^+$ 327.1, found 327.1.

N^4-(5-Chloro-[1,1':4',1''-terphenyl]-3-yl)-6-methylpyrimidine-2,4-diamine (99)

According to General Procedure D, bromo-pyrimidineamine **32** (0.3 g, 0.95 mmol) yielded

compound **99** as a tan solid (0.25 g, 69%); mp 104–105 °C. ^{1}H NMR (400 MHz, DMSO-d_6) δ

9.25 (s, 1H), 7.96 (t, J = 1.7 Hz, 1H), 7.84 (t, J = 1.7 Hz, 1H), 7.75 (s, 4H), 7.70 (d, J = 7.6 Hz,

2H), 7.46 (d, J = 7.6 Hz, 2H), 7.35 (m, 1H), 7.27 (t, J = 1.7 Hz, 1H), 6.27 (s, 2H), 5.88 (s, 1H),

2.09 (s, 3H). ^{13}C NMR (101 MHz, DMSO-d_6) δ 166.0, 163.3, 161.6 143.2, 142.0, 140.1, 139.9,

138.3, 134.2, 129. 5, 128.1, 127.7, 127.7, 127.0, 119.2, 117.7, 115.9, 95.8, 24.0. LC/MS (ESI)

calcd for $C_{23}H_{20}ClN_4$ (M + H)$^+$ 387.2, found 387.2.

N^4-(5-Chloro-4'-(dimethylamino)-[1,1'-biphenyl]-3-yl)-6-methylpyrimidine-2,4-diamine

(100) According to General Procedure D, bromo-pyrimidineamine **32** (0.3 g, 0.95 mmol) yielded

compound **100** as a yellow solid (0.28 g, 82%); mp 104–105 °C. ^{1}H NMR (400 MHz, Methanol-

d_4) δ 7.70 (t, J = 1.8 Hz, 1H), 7.51 (t, J = 1.8 Hz, 1H), 7.40 (d, J = 8.8 Hz, 2H), 7.12 (t, J = 1.8

Hz, 1H), 6.75 (d, J = 8.8 Hz, 2H), 5.91 (s, 1H), 2.90 (s, 6H), 2.14 (s, 3H). ^{13}C NMR (101 MHz,

Methanol-d_4) δ 165.0, 162.7, 161.9, 150.5, 143.2, 141.5, 134.2, 127.3, 127.0, 119.4, 117.0,

115.4, 112.6, 95.7, 39.3, 21.9. LC/MS (ESI) calcd for $C_{19}H_{21}ClN_5$ (M + H)$^+$ 354.2, found 354.2.

N^4-(2',5-Dichloro-[1,1'-biphenyl]-3-yl)-6-methylpyrimidine-2,4-diamine (101)

According to General Procedure D, bromo-pyrimidineamine **32** (0.3 g, 0.95 mmol) yielded compound **101** as an off-white solid (0.22 g, 66%); mp 83–84 °C. ^{1}H NMR (400 MHz, Methanol-d_4) δ 7.91 (m, 1H), 7.48 (m, 1H), 7.44 (t, J = 1.7 Hz, 1H), 7.37 – 7.30 (m, 3H), 6.99 (t, J = 1.7 Hz, 1H), 5.95 (s, 1H), 2.16 (s, 3H). ^{13}C NMR (101 MHz, Methanol-d_4) δ 165.1, 162.7, 161.9, 141.2, 141.2, 139.2, 133.5, 131.9, 130.9, 129.6, 128.9, 126.9, 122.5, 118.8, 118.5, 95.7, 21.8. LC/MS (ESI) calcd for $C_{17}H_{15}Cl_2N_4$ (M + H)$^+$ 345.1, found 345.1.

N^4-(3',5-Dichloro-[1,1'-biphenyl]-3-yl)-6-methylpyrimidine-2,4-diamine (102)

According to General Procedure D, bromo-pyrimidineamine **32** (0.3 g, 0.95 mmol) yielded compound **102** as an off-white solid (0.23 g, 71%); mp 169–170 °C. ^{1}H NMR (400 MHz, Methanol-d_4) δ 7.91 (m, 1H), 7.57 (t, J = 1.9 Hz, 1H), 7.54 (t, J = 1.9 Hz, 1H), 7.47 (m, 1H), 7.38 (t, J = 7.8 Hz, 1H), 7.33 (m, 1H), 7.15 (t, J = 1.9 Hz, 1H), 5.92 (s, 1H), 2.16 (s, 3H). ^{13}C NMR (101 MHz, Methanol-d_4) δ 165.1, 162.7, 161.8, 141.9, 141.7, 141.5, 134.5, 134.4, 130.0, 127.5, 126.5, 125.0, 120.1, 118.6, 116.2, 95.8, 21.9. LC/MS (ESI) calcd for $C_{17}H_{15}Cl_2N_4$ (M + H)$^+$ 345.1, found 345.1.

6-Methyl-N^4-(3',4',5-trichloro-[1,1'-biphenyl]-3-yl)pyrimidine-2,4-diamine (103)

According to General Procedure D, bromo-pyrimidineamine **32** (0.29 g, 0.93 mmol) yielded compound **103** as a yellow foam (0.27 g, 76%). ^{1}H NMR (400 MHz, CDCl$_3$) δ 7.55 (s, 1H), 7.49–7.42 (m, 2H), 7.34–7.27 (m, 2H), 7.20–7.09 (m, 2H), 5.94 (s, 1H), 5.18 (s, 2H), 2.21 (s, 3H). ^{13}C NMR (101 MHz, CDCl$_3$) δ 167.6, 162.7, 161.4, 141.0, 140.7, 139.4, 135.3, 133.0, 132.3, 130.8, 128.8, 126.2, 122.0, 120.5, 117.8, 95.2, 23.9. LC/MS (ESI) calcd for $C_{17}H_{14}Cl_3N_4$ (M + H)$^+$ 379.0, found 379.0.

(3',5-Dichloro-4'-fluoro-[1,1'-biphenyl]-3-yl)-6-methylpyrimidine-2,4-diamine (104)

According to General Procedure D, bromo-pyrimidineamine **32** (0.3 g, 0.95 mmol) yielded

compound **104** as an off-white solid (0.22 g, 64%); mp 129–130 °C. ^{1}H NMR (400 MHz,

Methanol-d_4) δ 7.90 (t, J = 1.8 Hz, 1H), 7.70 (m, 1H), 7.64 (t, J = 1.8 Hz, 1H), 7.56 (m, 1H),

7.31 (m, 1H), 7.19 (t, J = 1.8 Hz, 1H), 5.95 (s, 1H), 2.17 (s, 3H). LC/MS (ESI) calcd for

$C_{17}H_{14}Cl_2FN_4$ (M + H)$^+$ 363.1, found 363.1.

N^4-(4',5-Dichloro-3'-(trifluoromethyl)-[1,1'-biphenyl]-3-yl)-6-methylpyrimidine-2,4-diamine (105) According to General Procedure D, bromo-pyrimidineamine **32** (0.3 g, 0.95

mmol) yielded compound **105** as an off-white foam (0.22 g, 67%). ^{1}H NMR (500 MHz, DMSO-d_6) δ 9.34 (s, 1H), 8.07 (m, 1H), 8.01 (m, 2H), 7.91–7.78 (m, 2H), 7.39 (s, 1H), 6.32 (s, 2H), 5.91

(s, 1H), 2.13 (s, 3H). ^{13}C NMR (125 MHz, DMSO-d_6) δ 166.1, 163.2, 161.5, 143.36, 139.9,

138.9, 134.4, 134.3 132.9, 132.7, 126.4, 119.5, 118.4, 117.0, 116.2, 95.8, 24.0 (CF$_3$ carbon not

visible). LC/MS (ESI) calcd for $C_{18}H_{14}Cl_2F_3N_4$ (M + H)$^+$ 413.1, found 413.1.

N^4-(5-Chloro-3',5'-bis(trifluoromethyl)-[1,1'-biphenyl]-3-yl)-6-methylpyrimidine-2,4-diamine (106) According to General Procedure D, bromo-pyrimidineamine **32** (0.3 g, 0.95

mmol) yielded compound **106** as a tan solid (0.26 g, 61%); mp 159–160 °C. ^{1}H NMR (400

MHz, Methanol-d_4) δ 8.13 (s, 2H), 8.08 (t, J = 1.8 Hz, 1H), 7.96 (s, 1H), 7.67 (t, J = 1.8 Hz, 1H),

7.29 (t, J = 1.8 Hz, 1H), 5.94 (s, 1H), 2.17 (s, 3H). ^{13}C NMR (101 MHz, Methanol-d_4) δ 165.3,

162.7, 161.8, 142.3, 142.3, 139.7, 135.0, 131.9 (q, J_{CF} = 33.2 Hz), 127.1, 122.0, 121.0, 120.1,

119.4, 116.3, 95.9, 21.8. LC/MS (ESI) calcd for $C_{19}H_{14}ClF_6N_4$ (M + H)$^+$ 447.1, found 447.1.

N^4-(3-Chloro-5-(naphthalen-2-yl)phenyl)-6-methylpyrimidine-2,4-diamine (107)

According to General Procedure D, bromo-pyrimidineamine **32** (0.3 g, 0.95 mmol) yielded

compound **107** as tan solid (0.26 g, 75%); mp 189–190 °C. ^{1}H NMR (400 MHz, DMSO-d_6) δ

9.30 (s, 1H), 8.20 (m, 1H), 8.04 (t, J = 1.8 Hz, 1H), 8.02–7.96 (m, 2H), 7.94–7.88 (m, 2H), 7.80

(m, 1H), 7.56–7.47 (m, 2H), 7.37 (t, J = 1.8 Hz, 1H), 6.31 (s, 2H), 5.90 (s, 1H), 2.10 (s, 3H). ^{13}C

NMR (101 MHz, DMSO-d_6) δ 166.0, 163.3, 161.6, 143.3, 142.5, 136.7, 134.3, 133.7, 132.9,

129.0, 128.8, 127.9, 126.9, 126.8, 126.0, 125.4, 119.6, 117.8, 116.3, 95.8, 23.9. C/MS (ESI)

calcd for $C_{21}H_{18}ClN_4$ (M + H)$^+$ 361.1, found 361.1.

N^4-(3-Chloro-5-(phenanthren-9-yl)phenyl)-6-methylpyrimidine-2,4-diamine (108)

According to General Procedure D, bromo-pyrimidineamine **32** (0.3 g, 0.95 mmol) yielded

compound **108** as a white solid (0.28 g, 71%); mp 110–111 °C. ^{1}H NMR (400 MHz, Methanol-

d_4) δ 8.75 (d, J = 8.4 Hz, 1H), 8.69 (d, J = 8.4 Hz, 1H), 7.94 (s, 1H), 7.90–7.78 (m, 2H), 7.64–

7.46 (m, 6H), 7.05 (s, 1H), 5.89 (s, 1H), 2.12 (s, 3H). ^{13}C NMR (101 MHz, Methanol-d_4) δ

164.98, 162.6, 161.9, 142.6, 141.4, 137.2, 133.9, 131.3, 130.6, 130.4, 129.9, 128.4, 127.1, 126.6,

126.6, 126.3, 126.3, 126.1, 123.0, 122.7, 122.1, 119.2, 118.3, 95.8, 21.8. LC/MS (ESI) calcd for

$C_{25}H_{20}ClN_4$ (M + H)$^+$ 411.1, found 411.1.

N^4-(3-(Benzo[d][1,3]dioxol-5-yl)-5-chlorophenyl)-6-methylpyrimidine-2,4-diamine (109)

According to General Procedure D, bromo-pyrimidineamine **32** (0.3 g, 0.95 mmol) yielded

compound **109** a tan solid (0.27 g, 82%); mp 225–226 °C. ^{1}H NMR (400 MHz, DMSO-d_6) δ

9.18 (s, 1H), 7.93 (t, J = 2.0 Hz, 1H), 7.64 (t, J = 2.0 Hz, 1H), 7.20 (t, J = 2.0 Hz, 1H), 7.16–7.08

(m, 2H), 6.96 (m, 1H), 6.26 (s, 2H), 6.04 (s, 2H), 5.87 (s, 1H), 2.08 (s, 3H). ^{13}C NMR (101 MHz,

DMSO-d_6) δ 166.0, 163.3, 161.6, 148.4, 147.7, 143.0, 142.4, 134.0, 133.6, 121.0, 119.2, 117.3,

115.9, 109.1, 107.6, 101.7, 95.7, 23.9. LC/MS (ESI) calcd for $C_{18}H_{16}ClN_4O_2$ (M + H)$^+$ 355.1,

found 355.1.

N^4-(3-(Benzo[c][1,2,5]oxadiazol-5-yl)-5-chlorophenyl)-6-methylpyrimidine-2,4-diamine

(110) According to General Procedure E, bromo-pyrimidineamine **32** (0.3 g, 0.95 mmol) yielded

compound **110** as a yellow solid (0.24 g, 71%); mp 234–235 °C. ^{1}H NMR (400 MHz, DMSO-d_6)

δ 9.32 (s, 1H), 8.29 (d, J = 1.6 Hz, 1H), 8.12 (m, 1H), 8.05–7.96 (m, 2H), 7.93 (m, 1H), 7.42 (d,

J = 1.6 Hz, 1H), 6.34 (s, 2H), 5.89 (s, 1H), 2.10 (s, 3H). ^{13}C NMR (101 MHz, DMSO-d_6) δ

166.2, 163.3, 161.5, 149.9, 148.9, 143.3, 143.1, 140.3, 134.4, 133.8, 119.9, 119.0, 117.15, 116.7,

113.3, 95.8, 24.0. LC/MS (ESI) calcd for $C_{17}H_{14}ClN_6O$ (M + H)$^+$ 353.1, found 353.1.

N^4-(3-Chloro-5-(furan-3-yl)phenyl)-6-methylpyrimidine-2,4-diamine (111) According to

General Procedure E, bromo-pyrimidineamine **32** (0.30 g, 0.95 mmol) yielded compound **111** as

a white foam (0.21 g, 72%). ^{1}H NMR (400 MHz, DMSO-d_6) δ 9.17 (s, 1H), 8.24 (s, 1H), 7.91

(m, 1H), 7.72 (t, J = 1.8 Hz, 1H), 7.66 (t, J = 1.8 Hz, 1H), 7.21 (t, J = 1.8 Hz, 1H), 6.95 (m, 1H),

6.32 (s, 2H), 5.86 (s, 1H), 2.08 (s, 3H). ^{13}C NMR (101 MHz, DMSO-d_6) δ 165.9, 163.3, 161.6,

144.8, 143.2, 140.6, 134.5, 134.0, 125.4, 118.2, 117.1, 114.5, 109.2, 95.3, 23.9. LC/MS (ESI)

calcd for $C_{15}H_{14}ClN_4O$ (M + H)$^+$ 301.1, found 301.1.

N^4-(3-(Benzofuran-2-yl)-5-chlorophenyl)-6-methylpyrimidine-2,4-diamine (112)

According to General Procedure E, bromo-pyrimidineamine **32** (0.3 g, 0.95 mmol) yielded

compound **112** as an off-white foam (0.23 g, 69%). ^{1}H NMR (400 MHz, DMSO-d_6) δ 9.36 (s,

1H), 8.09 (t, J = 1.8 Hz, 1H), 8.01 (t, J = 1.8 Hz, 1H), 7.72–7.58 (m, 2H), 7.52 (s, 1H), 7.48 (t, J

= 1.8 Hz, 1H), 7.32 (t, J = 7.5 Hz, 1H), 7.25 (t, J = 7.5 Hz, 1H), 6.34 (s, 2H), 5.89 (s, 1H), 2.10

(s, 3H). ^{13}C NMR (101 MHz, DMSO-d_6) δ 166.1, 163.2, 161.5, 154.7, 154.2, 143.4, 134.4,

132.0, 129.1, 125.4, 123.8, 121.8, 118.6, 117.0, 113.4, 111.7, 103.7, 95.9, 23.4. LC/MS (ESI)

calcd for $C_{19}H_{15}ClN_4O$ (M + H)$^+$ 351.1, found 351.1.

N^4-(3-Chloro-5-(thiophen-3-yl)phenyl)-6-methylpyrimidine-2,4-diamine (113)

According to General Procedure E, bromo-pyrimidineamine **32** (0.3 g, 0.95 mmol) yielded

compound **113** as a yellow foam (0.22 g, 74%). ^{1}H NMR (400 MHz, DMSO-d_6) δ 9.21 (s, 1H),

7.97 (s, 1H), 7.92 (s, 1H), 7.78 (d, J = 2.2 Hz, 1H), 7.60 (m, 1H), 7.53 (s, 1H), 7.30 (d, J = 2.2

Hz, 1H), 6.34 (s, 2H), 5.89 (s, 1H), 2.10 (s, 3H). ^{13}C NMR (101 MHz, DMSO-d_6) δ 166.0, 163.3,

161.6, 143.2, 140.6, 137.5, 134.1, 127.7 126.6, 122.6, 118.76, 117.3, 115.2, 95.8, 23.9. LC/MS

(ESI) calcd for $C_{15}H_{14}ClN_4S$ (M + H)$^+$ 317.1, found 317.1.

N^4-(3-(Benzo[b]thiophen-2-yl)-5-chlorophenyl)-6-methylpyrimidine-2,4-diamine (114)

According to General Procedure E, bromo-pyrimidineamine **32** (0.3 g, 0.95 mmol) yielded

compound **114** as an off-white foam (0.21 g, 64%). ^{1}H NMR (400 MHz, DMSO-d_6) δ 9.35 (s,

1H), 8.01–7.90 (m, 4H), 7.84 (m, 1H), 7.38–7.34 (m, 3H), 6.31 (s, 2H), 5.89 (s, 1H), 2.10 (s,

3H). ^{13}C NMR (101 MHz, DMSO-d_6) δ 166.2, 163.2, 161.5, 143.4, 142.2, 140.7, 139.1, 135.8,

134.4, 125.4, 125.3, 124.5, 122.9, 121.6, 118.3, 118.2, 115.1, 95.9, 23.9. LC/MS (ESI) calcd for

$C_{19}H_{16}ClN_4S$ (M + H)$^+$ 367.1, found 367.1.

N^4-(3-Chloro-5-(thiazol-5-yl)phenyl)-6-methylpyrimidine-2,4-diamine (115) According

to General Procedure E bromo-pyrimidineamine **32** (0.30 g, 0.96 mmol) yielded compound **115**

as a yellow solid (0.25 g, 81%); mp 220–221 °C. ^{1}H NMR (400 MHz, DMSO-d_6) δ 9.29 (s, 1H),

9.09 (s, 1H), 8.36 (s, 1H), 7.95 (t, J = 1.8 Hz, 1H), 7.81 (t, J = 1.8 Hz, 1H), 7.30 (t, J = 1.8 Hz,

1H), 6.30 (s, 2H), 5.86 (s, 1H), 2.08 (s, 3H). ^{13}C NMR (101 MHz, DMSO-d_6) δ 166.1, 163.2,

161.4, 154.6, 143.4, 140.7, 137.8, 134.4, 133.0, 118.6, 118.2, 115.6, 95.8, 23.9. LC/MS (ESI)

calcd for $C_{14}H_{13}ClN_5S$ (M + H)$^+$ 318.1, found 318.1.

N^4-(3-Chloro-5-(1-methyl-1H-pyrazol-4-yl)phenyl)-6-methylpyrimidine-2,4-diamine

(116) According to General Procedure D, bromo-pyrimidineamine **32** (0.3 g, 0.95 mmol) yielded

compound **116** as a white solid (0.29 g, 88%); mp 204–205 °C. ^{1}H NMR (400 MHz, DMSO-d_6)

δ 9.13 (s, 1H), 8.15 (s, 1H), 7.98–7.79 (m, 2H), 7.54 (s, 1H), 7.15 (s, 1H), 6.29 (s, 2H), 5.85 (s,

1H), 3.84 (s, 3H), 2.08 (s, 3H). ^{13}C NMR (101 MHz, DMSO-d_6) δ 165.9, 163.23, 161.6, 143.2,

136.7, 135.1, 133.9, 128.8, 121.3, 117. 6, 116.1, 113.9, 95.7, 39.1, 23.9. LC/MS (ESI) calcd for

$C_{15}H_{16}ClN_6$ (M + H)$^+$ 315.1, found 315.1.

N^4-(3-Chloro-5-(pyrimidin-5-yl)phenyl)-6-methylpyrimidine-2,4-diamine (117)

According to General Procedure D, bromo-pyrimidineamine **32** (0.3 g, 0.95 mmol) yielded

compound **117** as a white solid (0.25 g, 84%); mp 184–185 °C. ^{1}H NMR (400 MHz, DMSO-d_6)

δ 9.32 (s, 1H), 9.19 (s, 1H), 9.10 (s, 2H), 7.99 (s, 1H), 7.90 (s, 1H), 7.39 (s, 1H), 6.33 (s, 2H),

5.87 (s, 1H), 2.08 (s, 3H). ^{13}C NMR (101 MHz, DMSO-d_6) δ 165.7, 161.7, 157.5, 155.0, 147.0,

146.0, 145.8, 142.9, 136.3, 119.8, 119.1, 116.1, 95.9, 22.5. LC/MS (ESI) calcd for $C_{15}H_{14}ClN_6$

(M + H)$^+$ 313.1, found 313.1.

N^4-(5-Ethyl-4'-fluoro-[1,1'-biphenyl]-3-yl)-6-methylpyrimidine-2,4-diamine (118)

According to General Procedure D, bromo-pyrimidineamine **38** (0.21 g, 0.70 mmol) yielded

compound **118** a tan oil (0.19 g, 83%). ^{1}H NMR (500 MHz, Methanol-d_4) δ 7.65–7.59 (m, 3H),

7.36 (t, J = 1.7 Hz, 1H), 7.19–7.13 (m, 2H), 7.10 (t, J = 1.7 Hz, 1H), 5.97 (s, 1H), 2.70 (q, J = 7.6

Hz, 2H), 2.18 (s, 3H), 1.29 (t, J = 7.6 Hz, 3H). ^{13}C NMR (126 MHz, Methanol-d_4) δ 164.8,

163.4, 162.3, 162.1 (d, J_{CF} = 162.1 Hz), 145.5, 140.7, 140.2, 137.5 (d, J_{CF} = 3.3 Hz), 128.4 (d,

J_{CF} = 8.0 Hz), 120.9, 119.0, 116.7, 115.0 (d, J_{CF} = 21.5 Hz), 95.2, 28.6, 21.9, 14.8. LC/MS (ESI)

calcd for $C_{19}H_{20}FN_4$ (M + H)$^+$ 323.2, found 323.2.

Biological Assays. *Materials.* Reagents were purchased from Sigma–Aldrich (St. Louis,

MO, USA) unless specified. *S*-Adenosyl-L-methionine (AdoMet) sulfate *p*-toluenesulfonate salt

was purchased from Affymetrix (Santa Clara, CA, USA), Gibco Iscove's modified Dulbecco's

medium (IMDM) was from Thermo Fisher Scientific (Waltham, MA, USA). Compound **1** was

kindly provided by Genzyme (now Sanofi-Genzyme, Waltham, MA, USA). Pyrimidineamine

compound stocks were made in dimethyl sulfoxide (DMSO), with an initial stock concentration

of 25 or 50 mM (or the highest achievable concentration for compounds with lower solubility).

Stocks were stored at –20 °C and thawed once to generate fresh solutions in DMSO for enzyme

and cell-based assays. DMSO based dilution series for the enzyme assays were generated using

Echo 555 acoustic liquid dispenser (Labcyte, Sunnyvale, CA, USA); final DMSO concentrations

in the assays were 2%. Cell growth inhibition was determined for a 3-fold serial dilution series

generated in DMSO so that final DMSO concentrations in the assay were 0.1%.

Protein Expression and Purification. Heterologous expression and purification of

recombinant *Tb*AdoMetDC/prozyme heterodimer and *Hs*AdoMetDC used in the enzyme activity

assays and for structure determination were carried out as previously described.[21, 47] The purified

*Tb*AdoMetDC/prozyme complex was concentrated to 73 mg/mL and stored at –80 °C.

Mass Spectrometry-Based AdoMetDC Activity Assay. The steady-state activity of

*Tb*AdoMetDC/prozyme and *Hs*AdoMetDC were measured using RapidFire–MS-based assay as

previously described.[22] Inhibition data were acquired in a concentration–response format based

on a 3-fold dilution series over the range from 0.01 µM to 180 µM final of inhibitor. Data were

normalized to a fully inhibited control (0.5 µM **1**) and fitted to the normalized response versus

log(inhibitor concentration) equation in *Prism* constraining bottom and Hill slope to 0 and –1,

respectively, to determine the IC_{50}.

Parasite Culture, Cell Viability Assay, and Western Blot Analysis. T. brucei brucei Lister

427 bloodstream-form parasites were cultured in HMI-19 medium supplemented with fetal

bovine serum (Atlanta Biologicals, Flowery Branch, GA, USA) in 96-well plates for the cell

viability assay or in culture flasks for the prozyme Western blot analysis, as previously

described.[22] Cell densities in the cell viability assay were analyzed using ATP–bioluminescence

assay with CellTiter-Glo reagent (Promega, Madison, WI, USA) after 48 h culturing in the

presence of serial dilutions of compound (ranging from 0.0038 to 25 µM or from 0.015 to 100

µM final in the assay) and at a fixed concentration of vehicle (0.1% DMSO) as previously

described.[22] The data were fitted to the normalized response versus log(inhibitor concentration)

equation in *Prism* constraining bottom to 0. Hill slope was constrained to –8 (based on the best-

fit value of a four-parameter fit in *Prism*) when the steepness of the curve resulted in a fit with an

ambiguous EC_{50} value (see Table S1). The Western blot analysis of prozyme levels in the treated

cell lysates was performed as previously described.[22]

In Vitro Metabolism and Distribution Analysis. Compound metabolic stability was assessed

using male CD-1 mouse and mixed-gender human hepatic microsomes as previously described.[22]

BBB permeability assay was done using MDCKII-hMDR1 monolayer cells as previously

described.[22]

X-ray Crystallography. *Protein Crystallization and Data Collection.*

*Tb*AdoMetDC/prozyme was diluted to final concentration of 4 mg/mL into a crystallization

buffer (50 mM bis-tris propane, pH 7.2, 50 mM NaCl, 4 mM tris(2-carboxyethyl)phosphine

(TCEP), 2 mM putrescine) containing 0.5 mM **44** added as 50 mM DMSO stock yielding a final

DMSO concentration of 1%. Protein and the inhibitor were allowed to equilibrate at room

temperature for 3 h, after which the sample was filtered at 23 °C using Ultrafree-MC 0.22 µm

PVDF centrifugal filter units (Merck Millipore, Tullagreen, Ireland). Crystals were obtained

using hanging-drop vapor diffusion method by combining 1 µL of the protein in crystallization

buffer, 1 µL of reservoir solution, and 0.5 µL of unliganded protein microseeds obtained using

Seed–Bead method (Hampton Research, Aliso Viejo, CA, USA) and diluted 50- fold as

previously described.[21] Reservoir solution contained 17% PEG 6000 and 100 mM bis-tris

propane, pH 7.0. Crystals formed on day 5 and were prepared for data collection by

cryoprotection in a combination of the crystallization buffer and reservoir solution supplemented

with 18% ethylene glycol. Crystals were then mounted and cryo-chilled in liquid nitrogen.

Diffraction data were collected at the Br K-edge at the Structure Biology Center at the Advance

Photon Source, Beamline 19-ID at 100 K(see Table S2). Data reduction was carried out by *HKL*

package.[48]

Structure Determination and Model Refinement. Previously solved atomic coordinates of

*Tb*AdoMetDC/prozyme (PDB identifier 5TVM)[21] were used as a search model for molecular

replacement in *Phaser*[49] as implemented in *Phenix* (v1.10.1-2155).[50] The coordinates and

geometry restraints for **44** were generated from a chemical formula in *Elbow*.[51] The ligand was

placed after initial positional refinement in *Phenix*[44] on the basis of $m\mathrm{F_o}-D\mathrm{F_c}$ positive density in

the active site and the anomalous diffraction map (Figure S1). The structure was further

improved through alternating manual model building in *Coot*[52] and positional, individual *B*-

factor, occupancy, and anomalous groups refinement in *Phenix*. Visualization of the atomic

coordinates and electron densities was done using *PyMOL* molecular graphics system (Version

1.8, Schrödinger).
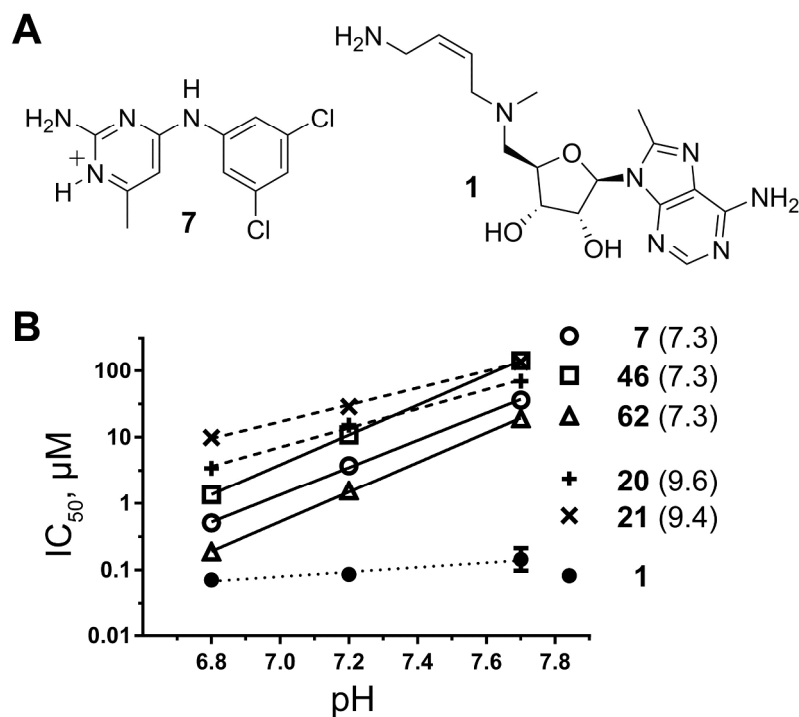
Figure 1. Pyrimidineamines are pH-dependent *Tb*AdoMetDC inhibitors. (**A**) Structure of the protonated form of pyrimidineamine **7** (N1 is predicted to have pK_a of 7.3), and structure of mechanism-based inhibitor Genz-644131 (**1**). (**B**) IC_{50} of pyrimidineamines plotted as a function of the assay buffer pH and fitted with linear regression analysis in *Prism* (GraphPad). Predicted $pK_a(N1)$ values are shown in parentheses. The slopes for pyrimidineamines with $pK_a(N1) = 7.3$ (solid lines) are compared with those for analogs with $pK_a(N1) > 9$ (dashed lines), and with that for a non-pyrimidineamine control (dotted line).
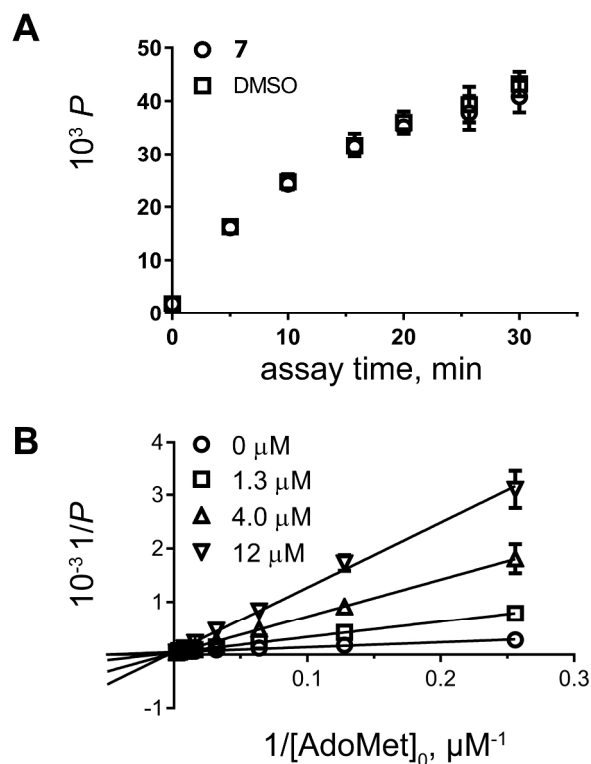
Figure 2. Mechanism of inhibition studies for **7**. (**A**) Evaluation of reversibility. Recovery of

enzyme activity after a 30 min incubation with inhibitor followed by a rapid 100-fold dilution of

the inhibitor. The progression of the reaction was measured as product formation using

RapidFire–MS analysis. (**B**) Determination of the inhibition modality. Double-reciprocal

Lineweaver-Burk plot of substrate titrations in the presence of four inhibitor concentrations

shows competitive inhibition.
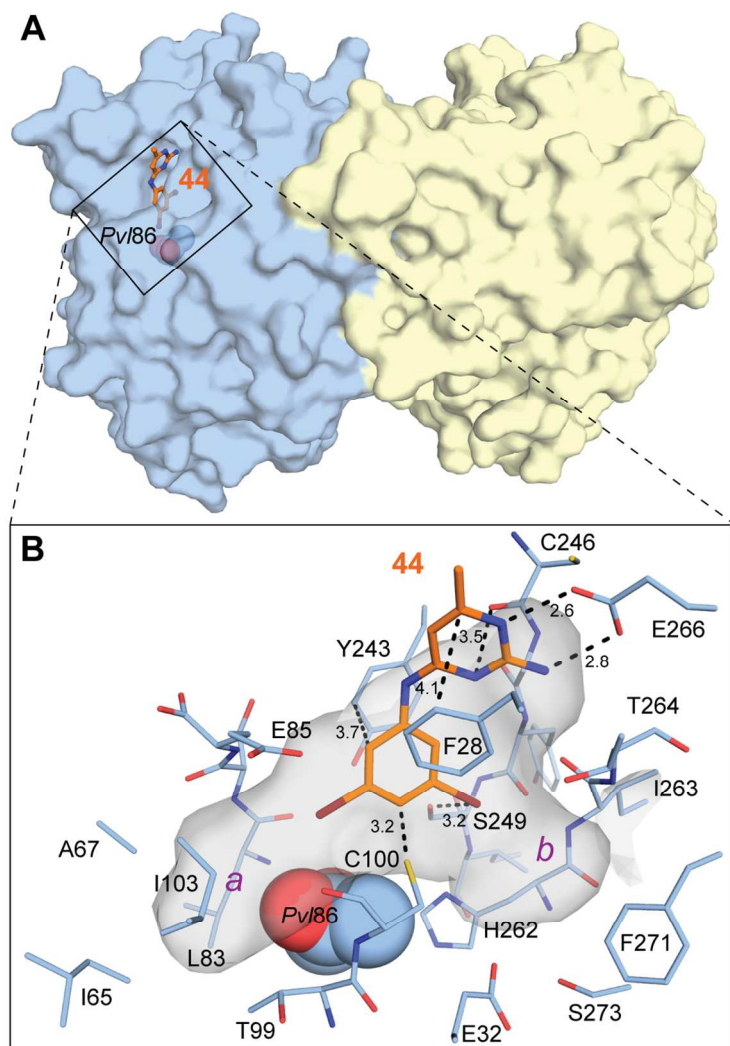
Figure 3. Crystal structure of *Tb*AdoMetDC/prozyme in complex with **44**. (**A**) Surface

representation of *Tb*AdoMetDC/prozyme (blue/yellow) with **44** (orange sticks) occupying the

catalytic site. Pyruvoyl residue (Pvl) is shown as spheres. (**B**) Surface representation of the

catalytic site. Residues forming the catalytic-site cavity are shown as sticks. Select interatomic

distances are shown as dashed lines with values in Å. The catalytic-site cavity is shown as a

semi-transparent gray surface. Two pockets that are partially occupied by bromines are labeled *a*

and *b* in purple.
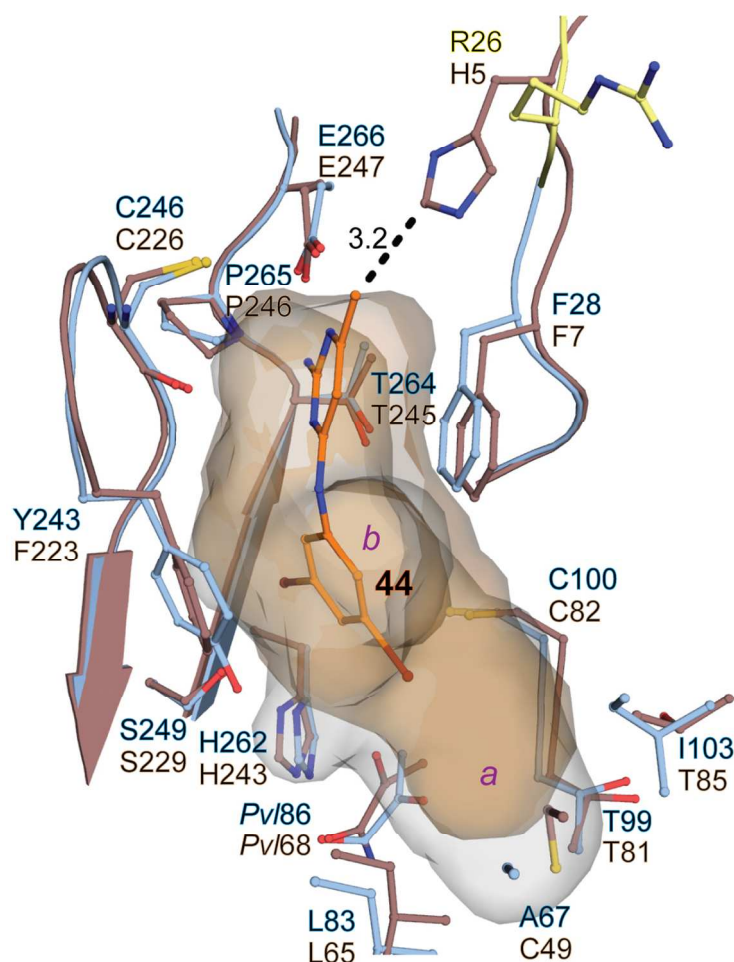
Figure 4. Comparison of human and *T. brucei* AdoMetDC active sites. Human AdoMetDC

(PDB 3DZ7, brown) was aligned with *Tb*AdoMetDC structure (blue) co-crystallized with **44**

(orange). The analogous residues are labeled in the corresponding colors (*T. brucei* residues on

top). Alignment was done in *PyMol*, and the side chains within 4 Å of an inhibitor (with the

exception of *Tb*Glu86/*Hs*Glu68) are shown here. A dashed line represents a distance, in Å,

between His5 of the human protein and **44** in the aligned *T. brucei* structure. Residues Ser25 and

Arg26, which were not modeled in **44**-liganded structure, are from the previously reported

unliganded *Tb*AdoMetDC structure (PDB 5TVM, yellow). The active-site cavities for human

(brown) and **44**-bound *T. brucei* (blue) AdoMetDCs are shown as semi-transparent surfaces

(pocket *b* is pointing away from the viewer).

	7	8	23	13	29	Controls	
						1	DMSO
$IC_{50\ (pH7.2)}$ (µM)	3.7	13	>180	>180	>180		
EC_{50} (µM)	5.6	9.9	27	8.9	>25		
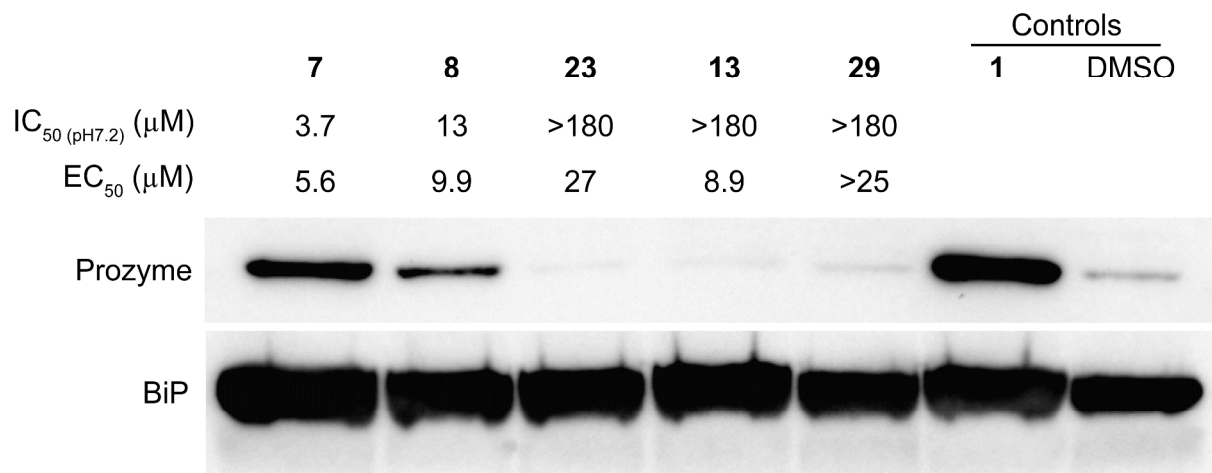
Figure 5. Mechanism of action studies in *T. brucei* bloodstream form parasites. Western blot analysis of prozyme levels in *T. brucei* cells treated with active or inactive pyrimidineamine analogs for 24 h. Three types of compounds were compared: 1) compounds that demonstrated low-micromolar inhibition of both *Tb*AdoMetDC at pH 7.2 ($IC_{50\ (pH7.2)}$) and of *T. brucei* cells in culture (EC_{50}) (**7** and **8**); 2) compounds that did not inhibit *Tb*AdoMetDC but did inhibit *T. brucei* cell growth (**23** and **13**); and 3) a compound that did not inhibit either *Tb*AdoMetDC or the cells (**29**). Cells were treated with $1.5 \times EC_{50}$ concentrations of inhibitors (or 30 µM **29**). *T. brucei* binding protein (BiP) was used as a loading control.

Supporting Information

Table S1 with structures and biological assay data for all tested compounds.

Table S2 with X-ray crystallography data collection and refinement statistics.

Figure S1 with electron density maps supporting ligand placement in the X-ray crystal structure.

Copies of H- and ^{13}C-NMR spectra of synthesized analogs.

Abbreviations

HAT, human African trypanosomiasis; AdoMet, *S*-adenosyl-L-methionine; AdoMetDC, *S*-adenosylmethionine decarboxylase; dcAdoMet, decarboxylated *S*-adenosyl-L-methionine; *Tb*, *T. brucei*; *Hs*, *Homo sapiens*; BBB, blood−brain barrier; CNS, central nervous system; NECT, nifurtimox−eflornithine combination therapy; HTS, high-throughput screening; SAR, structure−activity relationship; MS, mass spectrometry; Pgp, P-glycoprotein 1; DMSO, dimethyl sulfoxide; Pvl, pyruvoyl prosthetic group; PDB, Protein Data Bank.

Acknowledgements

Major datasets

The following dataset was generated and deposited:

Authors	Dataset title	Database information	Dataset URL
Volkov, O.A., Chen, Z., Phillips, M.A.	Crystal structure of *Trypanosoma brucei* AdoMetDC/prozyme heterodimer in complex with pyrimidineamine inhibitor **44**	Publicly available at the RCSB Protein Data Bank (accession number 6BM7)	http://www.rcsb.org/ pdb/explore/explore.do? structureId=6BM7

Authors will release the atomic coordinates and experimental data upon article publication.

References

(1) WHO: Neglected tropical diseases. http://www.who.int/neglected_diseases/diseases/en/ (accessed Jun 12, 2017).

(2) Kennedy, P. G. E. Clinical features, diagnosis, and treatment of human African trypanosomiasis (sleeping sickness). *Lancet Neurol.* **2013**, *12*, 186-194.

(3) Franco, J. R.; Simarro, P. P.; Diarra, A.; Jannin, J. G. Epidemiology of human African trypanosomiasis. *Clin. Epidemiol* **2014**, *6*, 257-275.

(4) WHO: Trypanosomiasis, human African (sleeping sickness). http://www.who.int/mediacentre/factsheets/fs259/en/ (accessed Jun 12, 2017).

(5) Franco, J. R.; Simarro, P. P.; Diarra, A.; Ruiz-Postigo, J. A.; Jannin, J. G. The journey towards elimination of gambiense human African trypanosomiasis: not far, nor easy. *Parasitology* **2014**, *141*, 748-760.

(6) Berthier, D.; Breniere, S. F.; Bras-Goncalves, R.; Lemesre, J. L.; Jamonneau, V.; Solano, P.; Lejon, V.; Thevenon, S.; Bucheton, B. Tolerance to trypanosomatids: a threat, or a key for disease elimination? *Trends Parasitol.* **2016**, *32*, 157-168.

(7) Capewell, P.; Cren-Travaille, C.; Marchesi, F.; Johnston, P.; Clucas, C.; Benson, R. A.; Gorman, T. A.; Calvo-Alvarez, E.; Crouzols, A.; Jouvion, G.; Jamonneau, V.; Weir, W.; Stevenson, M. L.; O'neill, K.; Cooper, A.; Swar, N. K.; Bucheton, B.; Ngoyi, D. M.; Garside, P.; Rotureau, B.; Macleod, A. The skin is a significant but overlooked anatomical reservoir for vector-borne African trypanosomes. *Elife* **2016**, *5*, e17716.

(8) Trindade, S.; Rijo-Ferreira, F.; Carvalho, T.; Pinto-Neves, D.; Guegan, F.; Aresta-Branco, F.; Bento, F.; Young, S. A.; Pinto, A.; Van Den Abbeele, J.; Ribeiro, R. M.; Dias, S.; Smith, T. K.;

Figueiredo, L. M. Trypanosoma brucei parasites occupy and functionally adapt to the adipose

tissue in mice. *Cell Host Microbe* **2016**, *19*, 837-848.

(9) Tanowitz, H. B.; Scherer, P. E.; Mota, M. M.; Figueiredo, L. M. Adipose tissue: a safe haven

for parasites? *Trends Parasitol.* **2017**, *33*, 276-284.

(10) Simarro, P. P.; Franco, J.; Diarra, A.; Postigo, J. a. R.; Jannin, J. Update on field use of the

available drugs for the chemotherapy of human African trypanosomiasis. *Parasitology* **2012**,

139, 842-846.

(11) Iten, M.; Mett, H.; Evans, A.; Enyaru, J. C.; Brun, R.; Kaminsky, R. Alterations in ornithine

decarboxylase characteristics account for tolerance of Trypanosoma brucei rhodesiense to D,L-

alpha-difluoromethylornithine. *Antimicrob. Agents Chemother.* **1997**, *41*, 1922-1925.

(12) Drugs for Neglected Diseases initiative: SCYX-7158 Oxaborole.

https://www.dndi.org/diseases-projects/portfolio/scyx-7158/ (accessed Jun 13, 2017).

(13) Drugs for Neglected Diseases initiative: Fexinidazole (HAT).

https://www.dndi.org/diseases-projects/portfolio/fexinidazole/ (accessed Jun 13, 2017).

(14) Jacobs, R. T.; Nare, B.; Phillips, M. A. State of the art in African trypanosome drug

discovery. *Curr. Top. Med. Chem.* **2011**, *11*, 1255-1274.

(15) Willert, E.; Phillips, M. A. Regulation and function of polyamines in African trypanosomes.

Trends Parasitol. **2012**, *28*, 66-72.

(16) Willert, E. K.; Phillips, M. A. Regulated expression of an essential allosteric activator of

polyamine biosynthesis in African trypanosomes. *PLoS Pathog.* **2008**, *4*, e1000183.

(17) Bacchi, C. J.; Brun, R.; Croft, S. L.; Alicea, K.; Buhler, Y. In vivo trypanocidal activities of

new S-adenosylmethionine decarboxylase inhibitors. *Antimicrob. Agents Chemother.* **1996**, *40*,

1448-1453.

(18) Bacchi, C. J.; Barker, R. H., Jr.; Rodriguez, A.; Hirth, B.; Rattendi, D.; Yarlett, N.; Hendrick, C. L.; Sybertz, E. Trypanocidal activity of 8-methyl-5'-{[(Z)-4-aminobut-2-enyl]-(methylamino)}adenosine (Genz-644131), an adenosylmethionine decarboxylase inhibitor. *Antimicrob. Agents Chemother.* **2009**, *53*, 3269-3272.

(19) Bitonti, A. J.; Byers, T. L.; Bush, T. L.; Casara, P. J.; Bacchi, C. J.; Clarkson, A. B.; Mccann, P. P.; Sjoerdsma, A. Cure of Trypanosoma brucei brucei and Trypanosoma brucei rhodesiense infections in mice with an irreversible inhibitor of S-adenosylmethionine decarboxylase. *Antimicrob. Agents Chemother.* **1990**, *34*, 1485-1490.

(20) Willert, E. K.; Fitzpatrick, R.; Phillips, M. A. Allosteric regulation of an essential trypanosome polyamine biosynthetic enzyme by a catalytically dead homolog. *Proc. Natl. Acad. Sci. U.S.A.* **2007**, *104*, 8275-8280.

(21) Volkov, O. A.; Kinch, L.; Ariagno, C.; Deng, X.; Zhong, S.; Grishin, N.; Tomchick, D. R.; Chen, Z.; Phillips, M. A. Relief of autoinhibition by conformational switch explains enzyme activation by a catalytically dead paralog. *Elife* **2016**, *5*, e20198.

(22) Volkov, O. A.; Cosner, C. C.; Brockway, A. J.; Kramer, M.; Booker, M.; Zhong, S.; Ketcherside, A.; Wei, S.; Longgood, J.; Mccoy, M.; Richardson, T. E.; Wring, S. A.; Peel, M.; Klinger, J. D.; Posner, B. A.; De Brabander, J. K.; Phillips, M. A. Identification of Trypanosoma brucei AdoMetDC inhibitors using a high-throughput mass spectrometry-based assay. *ACS Infect. Dis.* **2017**, *3*, 512-526.

(23) Valente, S.; Liu, Y.; Schnekenburger, M.; Zwergel, C.; Cosconati, S.; Gros, C.; Tardugno, M.; Labella, D.; Florean, C.; Minden, S.; Hashimoto, H.; Chang, Y.; Zhang, X.; Kirsch, G.; Novellino, E.; Arimondo, P. B.; Miele, E.; Ferretti, E.; Gulino, A.; Diederich, M.; Cheng, X.;

Mai, A. Selective non-nucleoside inhibitors of human DNA methyltransferases active in cancer including in cancer stem cells. *J. Med. Chem.* **2014**, *57*, 701-713.

(24) Borman, R. A.; Coleman, R. A.; Clark, K. L.; Oxford, A. W.; Hynd, G.; Archer, J. A.; Aley, A.; Harris, N. V. 5-HT2B Receptor Antagonists. Patent WO 2005/012263 A1, 2005.

(25) Sander, K.; Kottke, T.; Tanrikulu, Y.; Proschak, E.; Weizel, L.; Schneider, E. H.; Seifert, R.; Schneider, G.; Stark, H. 2,4-Diaminopyrimidines as histamine H4 receptor ligands--Scaffold optimization and pharmacological characterization. *Bioorg. Med. Chem.* **2009**, *17*, 7186-7196.

(26) Sekiya, K.; Takashima, H.; Ueda, N.; Kamiya, N.; Yuasa, S.; Fujimura, Y.; Ubasawa, M. 2-Amino-6-arylthio-9-[2-(phosphonomethoxy)ethyl]purine bis(2,2,2-trifluoroethyl) esters as novel HBV-specific antiviral reagents. *J. Med. Chem.* **2002**, *45*, 3138-3142.

(27) Medina, J. R.; Becker, C. J.; Blackledge, C. W.; Duquenne, C.; Feng, Y.; Grant, S. W.; Heerding, D.; Li, W. H.; Miller, W. H.; Romeril, S. P.; Scherzer, D.; Shu, A.; Bobko, M. A.; Chadderton, A. R.; Dumble, M.; Gardiner, C. M.; Gilbert, S.; Liu, Q.; Rabindran, S. K.; Sudakin, V.; Xiang, H.; Brady, P. G.; Campobasso, N.; Ward, P.; Axten, J. M. Structure-based design of potent and selective 3-phosphoinositide-dependent kinase-1 (PDK1) inhibitors. *J. Med. Chem.* **2011**, *54*, 1871-1895.

(28) Yi, B.; Long, S.; Gonzalez-Cestari, T. F.; Henderson, B. J.; Pavlovicz, R. E.; Werbovetz, K.; Li, C.; Mckay, D. B. Discovery of benzamide analogs as negative allosteric modulators of human neuronal nicotinic receptors: pharmacophore modeling and structure-activity relationship studies. *Bioorg. Med. Chem.* **2013**, *21*, 4730-4743.

(29) Wijtmans, M.; Scholten, D. J.; Roumen, L.; Canals, M.; Custers, H.; Glas, M.; Vreeker, M. C.; De Kanter, F. J.; De Graaf, C.; Smit, M. J.; De Esch, I. J.; Leurs, R. Chemical subtleties in

small-molecule modulation of peptide receptor function: the case of CXCR3 biaryl-type ligands. *J. Med. Chem.* **2012**, *55*, 10572-10583.

(30) Knapp, D. M.; Gillis, E. P.; Burke, M. D. A general solution for unstable boronic acids: slow-release cross-coupling from air-stable MIDA boronates. *J. Am. Chem. Soc.* **2009**, *131*, 6961-6963.

(31) Baell, J. B.; Holloway, G. A. New substructure filters for removal of pan assay interference compounds (PAINS) from screening libraries and for their exclusion in bioassays. *J. Med. Chem.* **2010**, *53*, 2719-2740.

(32) Mahar Doan, K. M.; Humphreys, J. E.; Webster, L. O.; Wring, S. A.; Shampine, L. J.; Serabjit-Singh, C. J.; Adkison, K. K.; Polli, J. W. Passive permeability and P-glycoprotein-mediated efflux differentiate central nervous system (CNS) and non-CNS marketed drugs. *J. Pharmacol. Exp. Ther.* **2002**, *303*, 1029-1037.

(33) Copeland, R. A. *Evaluation of Enzyme Inhibitors in Drug Discovery : a Guide for Medicinal Chemists and Pharmacologists*. Wiley-Interscience: Hoboken, N.J., 2005.

(34) Zhang, Y.; Skolnick, J. TM-align: a protein structure alignment algorithm based on the TM-score. *Nucleic Acids Res.* **2005**, *33*, 2302-2309.

(35) Duan, G.; Smith, V. H.; Weaver, D. F. Characterization of aromatic-thiol π-type hydrogen bonding and phenylalanine-cysteine side chain interactions throughab initiocalculations and protein database analyses. *Mol. Phys.* **2001**, *99*, 1689-1699.

(36) Meyer, E. A.; Castellano, R. K.; Diederich, F. Interactions with aromatic rings in chemical and biological recognition. *Angew. Chem. Int. Ed. Engl.* **2003**, *42*, 1210-1250.

(37) Cavallo, G.; Metrangolo, P.; Milani, R.; Pilati, T.; Priimagi, A.; Resnati, G.; Terraneo, G. The halogen bond. *Chem. Rev.* **2016**, *116*, 2478-2601.

(38) Mccloskey, D. E.; Bale, S.; Secrist, J. A., 3rd; Tiwari, A.; Moss, T. H., 3rd; Valiyaveettil, J.; Brooks, W. H.; Guida, W. C.; Pegg, A. E.; Ealick, S. E. New insights into the design of inhibitors of human S-adenosylmethionine decarboxylase: studies of adenine C8 substitution in structural analogues of S-adenosylmethionine. *J. Med. Chem.* **2009**, *52*, 1388-1407.

(39) Xiao, Y.; Nguyen, S.; Kim, S. H.; Volkov, O. A.; Tu, B. P.; Phillips, M. A. Product feedback regulation implicated in translational control of the Trypanosoma brucei S-adenosylmethionine decarboxylase regulatory subunit prozyme. *Mol. Microbiol.* **2013**, *88*, 846-861.

(40) Vincent, I. M.; Creek, D.; Watson, D. G.; Kamleh, M. A.; Woods, D. J.; Wong, P. E.; Burchmore, R. J.; Barrett, M. P. A molecular mechanism for eflornithine resistance in African trypanosomes. *PLoS Pathog.* **2010**, *6*, e1001204.

(41) Bitonti, A. J.; Dumont, J. A.; Mccann, P. P. Characterization of Trypanosoma brucei brucei S-adenosyl-L-methionine decarboxylase and its inhibition by Berenil, pentamidine and methylglyoxal bis(guanylhydrazone). *Biochem. J.* **1986**, *237*, 685-689.

(42) Brun, R.; Buhler, Y.; Sandmeier, U.; Kaminsky, R.; Bacchi, C. J.; Rattendi, D.; Lane, S.; Croft, S. L.; Snowdon, D.; Yardley, V.; Caravatti, G.; Frei, J.; Stanek, J.; Mett, H. In vitro trypanocidal activities of new S-adenosylmethionine decarboxylase inhibitors. *Antimicrob. Agents Chemother.* **1996**, *40*, 1442-1447.

(43) Tolbert, W. D.; Zhang, Y.; Cottet, S. E.; Bennett, E. M.; Ekstrom, J. L.; Pegg, A. E.; Ealick, S. E. Mechanism of human S-adenosylmethionine decarboxylase proenzyme processing as revealed by the structure of the S68A mutant. *Biochemistry* **2003**, *42*, 2386-2395.

(44) Bale, S.; Brooks, W.; Hanes, J. W.; Mahesan, A. M.; Guida, W. C.; Ealick, S. E. Role of the sulfonium center in determining the ligand specificity of human S-adenosylmethionine decarboxylase. *Biochemistry* **2009**, *48*, 6423-6430.

(45) Bale, S.; Lopez, M. M.; Makhatadze, G. I.; Fang, Q.; Pegg, A. E.; Ealick, S. E. Structural basis for putrescine activation of human S-adenosylmethionine decarboxylase. *Biochemistry* **2008**, *47*, 13404-13417.

(46) Shantz, L. M.; Stanley, B. A.; Secrist, J. A.; Pegg, A. E. Purification of human S-adenosylmethionine decarboxylase expressed in Escherichia coli and use of this protein to investigate the mechanism of inhibition by the irreversible inhibitors, 5'-deoxy-5'-[(3-hydrazinopropyl)methylamino]adenosine and 5'-{[(Z)-4-amino-2-butenyl]methylamino}-5'-deoxyadenosine. *Biochemistry* **1992**, *31*, 6848-6855.

(47) Beswick, T. C.; Willert, E. K.; Phillips, M. A. Mechanisms of allosteric regulation of Trypanosoma cruzi S-adenosylmethionine decarboxylase. *Biochemistry* **2006**, *45*, 7797-7807.

(48) Minor, W.; Cymborowski, M.; Otwinowski, Z.; Chruszcz, M. HKL-3000: the integration of data reduction and structure solution - from diffraction images to an initial model in minutes. *Acta Crystallogr. D Biol. Crystallogr.* **2006**, *62*, 859-866.

(49) Mccoy, A. J.; Grosse-Kunstleve, R. W.; Adams, P. D.; Winn, M. D.; Storoni, L. C.; Read, R. J. Phaser crystallographic software. *J. Appl. Crystallogr.* **2007**, *40*, 658-674.

(50) Adams, P. D.; Afonine, P. V.; Bunkoczi, G.; Chen, V. B.; Davis, I. W.; Echols, N.; Headd, J. J.; Hung, L. W.; Kapral, G. J.; Grosse-Kunstleve, R. W.; Mccoy, A. J.; Moriarty, N. W.; Oeffner, R.; Read, R. J.; Richardson, D. C.; Richardson, J. S.; Terwilliger, T. C.; Zwart, P. H. PHENIX: a comprehensive Python-based system for macromolecular structure solution. *Acta Crystallogr. D Biol. Crystallogr.* **2010**, *66*, 213-221.

(51) Moriarty, N. W.; Grosse-Kunstleve, R. W.; Adams, P. D. Electronic Ligand Builder and

Optimization Workbench (eLBOW): a tool for ligand coordinate and restraint generation. *Acta*

Crystallogr. D Biol. Crystallogr. **2009**, *65*, 1074-1080.

(52) Emsley, P.; Lohkamp, B.; Scott, W. G.; Cowtan, K. Features and development of Coot. *Acta*

Crystallogr. D Biol. Crystallogr. **2010**, *66*, 486-501.

For Table of Contents Only